Soil Dynamics and Earthquake Engineering 129 (2020) 105925

Contents lists available at ScienceDirect

Soil Dynamics and Earthquake Engineering

journal homepage: http://www.elsevier.com/locate/soildyn

Seismic drift response of seesaw-braced and buckling-restrained braced steel structures: A comparison study

Panagiota S. Katsimpini, Paraskevi K. Askouni, George A. Papagiannopoulos *, Dimitris L. Karabalis

Department of Civil Engineering, University of Patras, Greece

ARTICLE INFO

Keywords:
Seesaw system
Buckling-restrained braces
Steel structures
Seismic drifts
Soil-structure interaction
Angle of seismic incidence

ABSTRACT

A numerical comparison study of the interstorey and the residual interstorey seismic drifts of steel structures equipped with the seesaw system and buckling-restrained braces is carried out. This investigation involves inelastic time-history seismic analyses of 2-, 5- and 8-storey 3-D steel structures, with specific orientation of columns and configuration of braces, for the design basis earthquake. The effects of soil-structure interaction and seismic incident angle are also considered in these analyses. Comparison of the seismic drift responses experienced by the seesaw-braced and the buckling-restrained braced steel structures, reveals different peak interstorey drift values but in many cases similar drift concentration along the height of the structures. Furthermore, the seesaw-braced steel structures exhibit, in general, larger peak residual drifts than buckling-restrained braced steel structures.

1. Introduction

After a major seismic event, the integrity of a structure, e.g. its capacity for immediate occupancy, should be certified via the explicit consideration of seismic response indexes such as the peak drifts. Focusing on steel structures, several studies, e.g. Ref. [1], have demonstrated the necessity to consider residual (permanent) drifts after an earthquake. Residual drifts, i.e. permanent drifts caused by yielding, permit the evaluation of the seismic performance of a steel structure regarding deformation and damage to its elements. In regions where repeated earthquakes can take place in a short period of time, the occurrence of a second or a third earthquake (not necessarily aftershocks of the first earthquake), increases the collapse risk of a steel structure if its residual drifts are significant [2]. The importance of residual drift has been also recognized as a key design parameter of novel seismic force resisting systems for steel structures, e.g., Refs. [3,4]. The limit value of 0.5% for residual drifts has been established as the threshold beyond which any repair of a structure is unfeasible in comparison to its rebuilding [5].

Over the past 20 years, buckling-restrained braces (BRBs) have shown an increased popularity in China, Japan, Taiwan, United States and other countries, as a primary force-resisting system for steel structures [6]. More recently, BRBs have also been applied for the seismic retrofit of older non-ductile structures [7]. BRBs, due to their stable and symmetric cyclic hysteretic response, have the advantage of developing full plastic strength in both tension and compression, providing, thus, significant energy dissipation and ductility without exhibiting strength degradation. The main disadvantage associated with BRBs is their tendency to cause storey drift concentration, i.e. accumulation of significant storey drifts in a few storeys without a more or less "uniform" distribution along the height of a structure, which inevitably leads to large residual storey drifts [8]. The reason behind these drift issues is the low post-yield stiffness of the BRBs. In an effort to improve the seismic drift behavior of steel structures with BRBs, back-up moment resisting frames [9], different beam-to-column connections [10] and fixed base columns [11] have been used. Nevertheless, the drift issues are certainly decisive for both the design basis and maximum credible earthquakes, and strongly influence the seismic collapse performance of buckling-restrained braced steel structures [8,12–14]. Detailed design requirements for steel structures with BRBs are provided in Refs. [15–17]. EC 8 [18] does not provide yet any procedure for the design of steel structures with BRBs, even though some works, e.g. Ref. [19], have proposed design procedures in accordance with its framework.

A shift in the philosophy of seismic force resisting systems for steel structures, i.e., from BRBs to self-centering braces and tension-only braces, has been recently noticed. Among the various self-centering

* Corresponding author.
E-mail address: gpapagia@upatras.gr (G.A. Papagiannopoulos).

https://doi.org/10.1016/j.soildyn.2019.105925
Received 6 October 2019; Received in revised form 22 October 2019; Accepted 25 October 2019
Available online 4 November 2019
0267-7261/© 2019 Elsevier Ltd. All rights reserved.

and tension-only braces proposed so far, e.g. Refs. [20–24], the noticeable performance of the seesaw system towards the mitigation of the seismic response of steel structures has been highlighted in Refs. [25–29]. From the seismic response results of seesaw-braced low-rise steel structures presented in Refs. [28,29], the main problem observed is that of the possible failure of the spiral strand ropes (their tensile strength is exceeded) beyond the design basis earthquake. This failure is responsible for residual drifts in excess of the threshold 0.5% value.

The purpose of this work is to compare the interstorey drift (IDR) and residual interstorey drift (RIDR) responses of low-rise seesaw-braced and buckling-restrained braced steel structures using inelastic time-history seismic analyses. In particular, 2-, 5- and 8-storey 3-D steel structures designed with both the seesaw system or with BRBs are subjected to a number of recorded seismic motions that represent the design basis earthquake. The steel structures have specific orientation of columns and configuration of braces. Effects of soil-structure interaction and of seismic incident angle are also considered in these analyses. The seismic drift response results presented include only those analyses in which certain conditions regarding the seismic performance of steel structures are satisfied. These conditions depend on the values of the axial displacement of the BRBs, the tensile force of the spiral strand ropes, the axial compression in columns of the lowest storey, as well as on the level of acceptable plastic hinge rotations for beams and columns which precede the formation of a soft-storey mechanism.

Comparison of the seismic drift responses experienced by the steel structures for both bracing types examined, reveals different peak IDR values but in many cases similar drift concentration. The peak RIDRs seem to be more critical for the seesaw-braced than for buckling-restrained braced steel structures. It should be noted that the results of the drift responses presented in this study, and, therefore, the attempted comparison study between the two bracing systems, depends on the orientation (layout) of the columns as well as on the position and configuration of the braces. Therefore, the drift results presented herein are only indicative of the steel structures studied, but certainly offer a clue towards the seismic behavior (or performance) of these special types of braced steel structures.

2. Seismic analysis of 3-D steel structures

The 2-, 5- and 8-storey seesaw-braced and buckling-restrained braced steel structures considered herein have a square plan configuration of 18 × 18 m, storey heights of 3.0 m and bay spacing of 6.0 m in each direction. The column orientation is shown in Fig. 1. Diaphragm action is assumed at every floor due to the presence of a composite slab. Dead and live loads on the composite slabs are 8.0 kN/m^2 and 3.0 kN/m^2, respectively. The steel structures are initially designed as typical concentrically braced frames according to EC 3 [30] and EC 8 [18] with fixed base. The design seismic load is calculated using the design spectrum of EC 8 [18] that corresponds to peak ground acceleration (PGA) of 0.36 g, soil type B and behavior factor equal to 3. The storey shear computed from spectrum analysis is used in order to estimate: i) the diameter of the spiral strand ropes for the seesaw-braced steel structures and ii) the cross-section area of the core of the BRB for the buckling-restrained braced structures. Effects of accidental torsion are omitted. The stability coefficient is computed at every storey of the steel structures and it is checked according to EC 8 [18]. A 20.0 m × 20.0 m rigid mat foundation is designed with depth 0.3 m, 0.6 m and 0.8 m for the 2-, 5- and 8-storey steel structures, respectively. Soil-structure interaction (SSI) effects are taken into account for soil types C and D.

2.1. Seesaw-braced steel structures

A typical seesaw system installed in a steel frame is shown in Fig. 2. The 2-, 5- and 8-storey seesaw-braced steel structures are shown in Fig. 3. The spiral strand ropes (shown with green colour in Fig. 3) are anchored at both ends of the perimeter beams, at the same floor level,

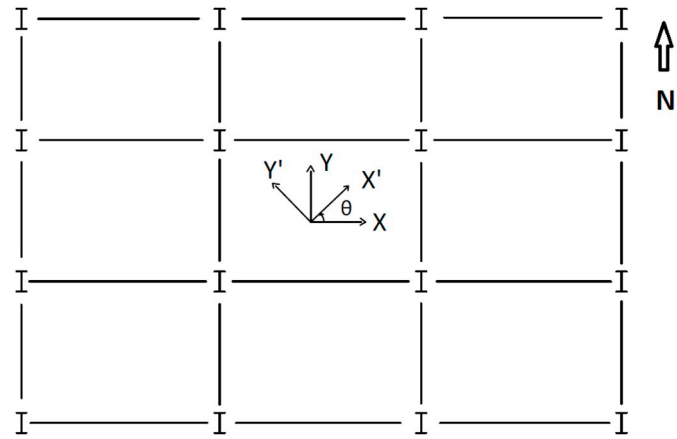

Fig. 1. Orientation of columns for the 2-, 5- and 8-storey seesaw-braced and buckling-restrained braced steel structures.

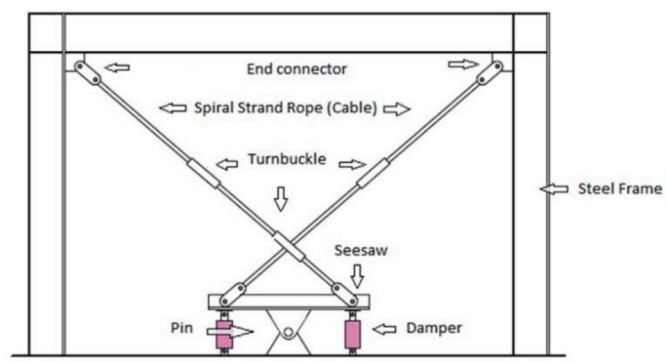

Fig. 2. The seesaw system installed in a steel frame.

and the seesaw device (involving the seesaw plates and linear viscous dampers) is installed at the middle bay of the perimeter frames. All the seesaw devices are considered to be centrally placed within the perimeter frame, in order to avoid any eccentricity issues.

A pretension is applied to the spiral strand ropes (about 10% of their tensile breaking strength) and it is also assumed that their anchorage type is such that the tensile breaking strength values do not need to be reduced [31]. The gusset plates for the anchorage of the spiral strand ropes are not modelled in order to keep the analyses simple and to avoid the introduction of several parameters associated with their modelling, e.g., welds, buckling, etc. Vertically positioned linear viscous dampers (clevis-clevis configuration) with a damping coefficient of 250 kN/m are utilized. Due to the mid-stroke length of these dampers, the height of the vertical steel plates of the seesaw is 870 mm. The length of the horizontal steel plate of the seesaw is 1600 mm.

The steel grade used is S235 for beams and S355 for columns and seesaw plates. All connections of steel members are moment-resisting ones except those of the secondary beams (interior beams at floor levels that are not part of a frame) that are pinned. The design of the seesaw-braced steel structures is performed by SAP 2000 [32]. Final sections for columns, beams and for the diameter and the design tensile breaking strength of the spiral strand ropes are mentioned in Table 1. Referring to Fig. 3, the same diameter of spiral strand ropes is used in both NS and EW directions of the seesaw-braced steel structures.

2.2. Buckling-restrained braced steel structures

The 2-, 5- and 8-storey buckling-restrained braced steel structures

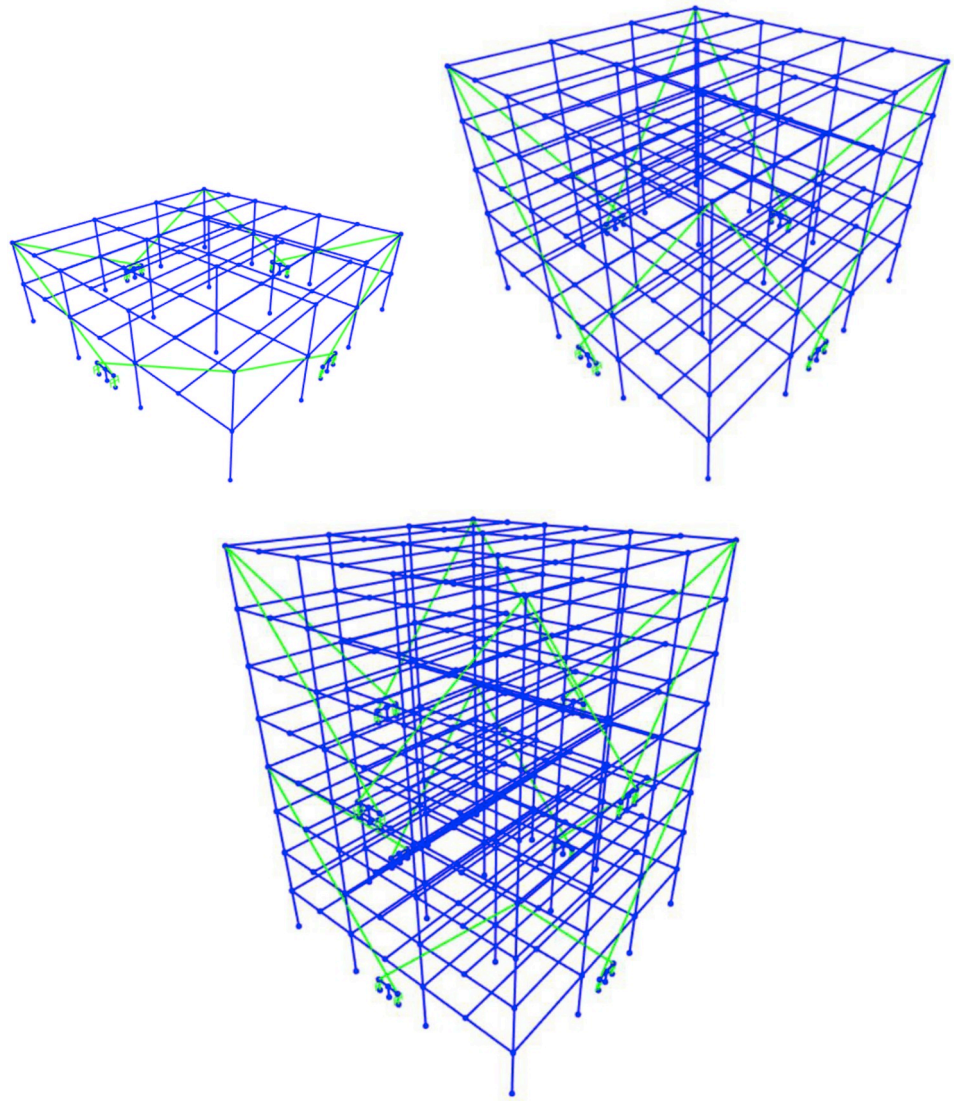

Figure 3. 2-, 5-, 8-storey seesaw-braced steel structures.

Table 1
Sections of beams & columns, diameters and design tensile breaking strengths of the spiral strand ropes.

Steel structure	Beams	Columns	Diameter (mm)	Breaking strength (kN)
2-storey	IPE 450	HEM 320	50	1560
5-storey	IPE 500	HEM 600	110	7570
8-storey	IPE 500	HEM 700	115	8270

are shown in Fig. 4. BRBs (shown with green colour in Fig. 4) are installed at the middle bay of the perimeter frames in a chevron configuration. To account for the relative stiffness of core plate transitions, brace end connections and gusset plate connections, the cross-section area of the core of the BRB is modified following Ref. [33]. The gusset plate connections of the BRB-to-beam and of the BRB-to-column are not modelled in order to keep the analyses simple and to avoid the introduction of several parameters associated with their modelling, e.g., welds, buckling, etc. The design axial displacement which the BRB should accommodate is two times the design storey drift (2%), i.e., 0.084 m. On the basis of this axial displacement, the strain hardening adjustment and compression overstrength factors are used to define the ultimate tensile and compressive yield strengths of the BRBs. Beams and columns are then proportioned employing these factors in order to remain elastic [16].

The steel grade used is S235 for beams and BRBs and S355 for columns. All connections of steel members are moment-resisting ones except those of the secondary beams (interior beams at floor levels that are not part of a frame) that are pinned. The ends of the BRBs are also considered pinned. The program ETABS [34] is used for the design of the buckling-restrained braced steel structures, where commercial BRB sections are available. The chosen sections for columns and beams and the area of the BRB core are mentioned in Table 2. Referring to Fig. 4, the area of the core of the BRBs is different in the NS and EW directions of the buckling-restrained braced steel structures.

2.3. Inclusion of soil-structure interaction

The effects of soil-structure interaction (SSI) are included in the following analyses via a discrete system of frequency independent springs, dashpots and masses which effectively replace the mat foundation and its surrounding soil, as reported in Ref. [35]. This discrete system takes approximately into account the horizontal and vertical

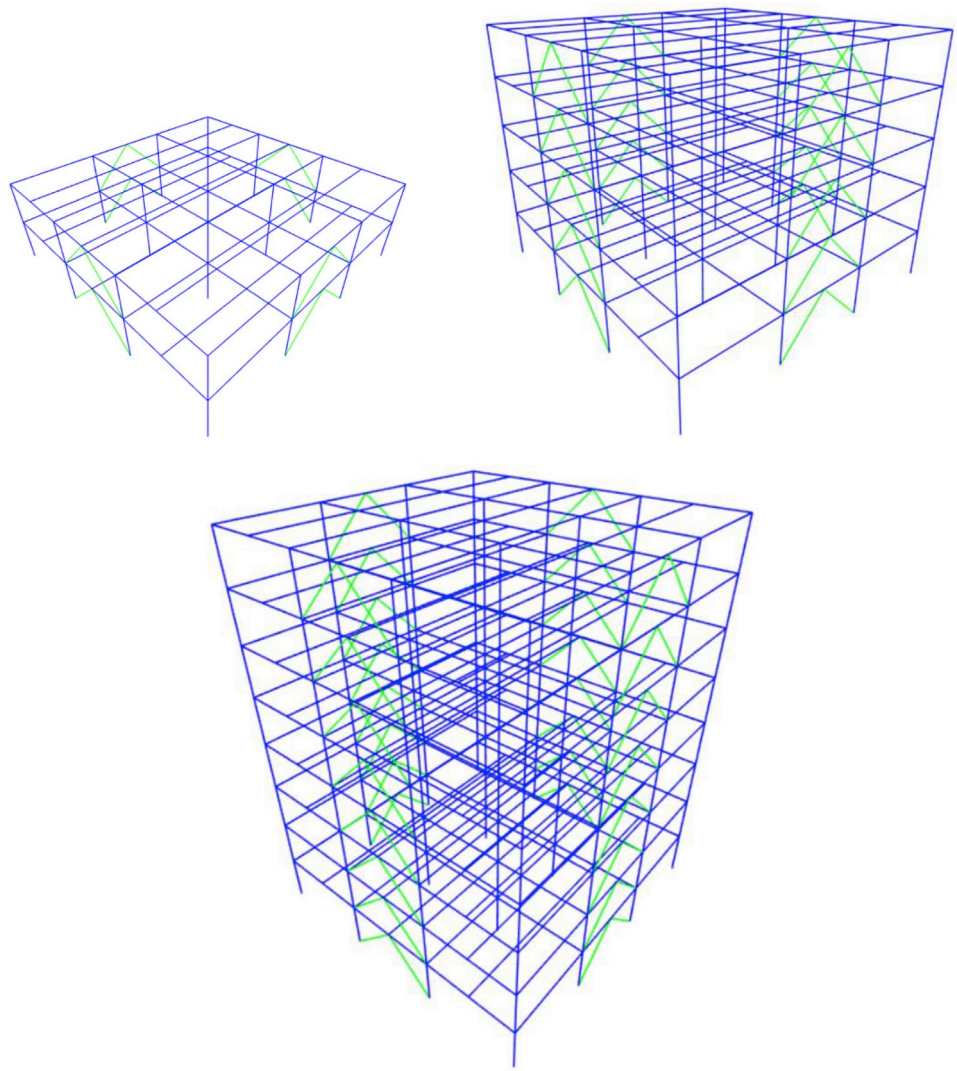

Fig. 4. 2-, 5-, 8-storey buckling-restrained braced steel structures.

Table 2
Sections of beams, columns and BRB core.

Steel structure	Beams	Columns	Direction: Storey/BRB core (in cm^2)
2-storey	IPE 450	HEM 320	NS & EW: 1st/32, 2nd/23
5-storey	IPE 500	HEM 600	EW: 1st/55, 2nd/52, 3rd/45, 4th/32, 5th/23 NS: 1st/39, 2nd/35, 3rd/29, 4th/23, 5th/19
8-storey	IPE 500	HEM 700	EW: 1st/55, 2nd/52, 3rd/48, 4th/42, 5th/39, 6th/32, 7th/26, 8th/16 NS: 1st/39, 2nd/35, 3rd/32, 4th/29, 5th/26, 6th/23, 7th/19, 8th/13

translations as well as the rocking and torsion of a rigid mat foundation resting on a homogeneous half space. However, it cannot handle non-linear effects like uplift of the foundation.

For the cases of soil types and structures studied herein, inertial SSI effects are dominant and, thus, kinematic effects may be neglected. In comparison to soft and very soft soils (soil types C and D), SSI effects for stiffer soils (soil type B) are small and, thus, they can be neglected, e.g. see Ref. [36].

The values for the springs, dashpots and masses of the aforementioned discrete system are calculated utilizing the formulas provided in Ref. [35]. These values correspond to linear soil behavior but can be turned into equivalent linear ones following the recommendations of EC 8 in consideration of the anticipated soil nonlinearity at strong ground motions [36]. In particular, the shear modulus of soil types C and D is obtained using a shear wave velocity equal to 270 m/sec and 180 m/sec and a soil density equal to 1800kgr/m^3 and 1900kgr/m^3, respectively. The shear modulus is then conservatively reduced to 16% of its initial value in order to take into account the development of non-linear soil deformations in soil types C and D for large levels of ground acceleration. Due to the aforementioned reduction of the shear modulus of soil types C and D, the shear wave velocity of these soil types is less than 100 m/sec, which is in accordance to the SSI consideration requirement of EC 8 [36]. According to Ref. [35], only one such discrete system is needed to model a rigid mat foundation. This discrete system originates from the geometric centre of the mat foundation (geometric centre of the framing system of Fig. 1) and it is connected to the lower end of all steel columns (including the vertical members of the seesaw system for the seesaw-braced steel structures) via horizontal rigid elements.

The steel structures of Figs. 3 and 4 are then dimensioned for the design spectrum of EC 8 [18] and soil types C and D, with PGA 0.36 g and behavior factor 3. The thus calculated geometric properties of the steel structures founded on soil types C and D are the same as those in Tables 1–2 (corresponding to soil type B), even though the stress ratio of

Table 3
Modal properties of steel structures (soil type B).

Steel structure	Mode number	Period (sec)	Mass participation – Translation x	Mass participation – Translation y	Mass participation – Torsion z
2-storey seesaw-braced	1	0.458	0	0.898	0
	2	0.342	0.865	0	0
	3	0.324	0	0	0.875
2-storey with BRBs	1	0.253	0	0.818	0
	2	0.212	0.884	0	0
	3	0.149	0	0	0.895
5-storey seesaw-braced	1	1.053	0	0.845	0
	2	0.671	0.781	0	0
	3	0.666	0	0	0.795
	4	0.344	0	0.098	0
	5	0.198	0	0	0.120
	6	0.192	0.129	0	0
5-storey with BRBs	1	0.513	0	0.810	0
	2	0.424	0.790	0	0
	3	0.314	0	0	0.788
	4	0.188	0	0.078	0
	5	0.165	0	0	0.117
	6	0.140	0.135	0	0
8-storey seesaw-braced	1	1.658	0	0.835	0
	2	1.086	0.774	0	0
	3	1.053	0	0	0.791
	4	0.535	0	0.091	0
	5	0.302	0	0	0.084
	6	0.276	0.078	0	0
8-storey with BRBs	1	0.854	0	0.774	0
	2	0.724	0.757	0	0
	3	0.533	0	0	0.751
	4	0.293	0	0.144	0
	5	0.231	0.141	0	0
	6	0.179	0	0	0.150

Table 4
Modal properties of steel structures (soil type C).

Steel structure	Mode number	Period (sec)	Mass participation – Translation x	Mass participation – Translation y	Mass participation – Rocking x	Mass participation – Rocking y	Mass participation – Torsion z
2-storey seesaw-braced	1	0.617	0	0.638	0.285	0	0
	2	0.580	0	0	0	0	0.887
	3	0.572	0.594	0	0	0.362	0
	4	0.266	0	0.070	0.594	0	0
	5	0.264	0.134	0	0	0.527	0
2-storey with BRBs	1	0.561	0	0.767	0.333	0	0
	2	0.530	0.698	0	0	0.409	0
	3	0.466	0	0	0	0	0.790
	4	0.259	0	0.124	0.474	0	0
	5	0.249	0.182	0	0	0.396	0
5-storey seesaw-braced	1	1.453	0	0.663	0.384	0	0
	2	1.213	0.614	0	0	0.464	0
	3	0.956	0	0	0	0	0.887
	4	0.403	0	0.120	0.404	0	0
	5	0.350	0.023	0	0	0.120	0
	6	0.311	0.138	0	0	0.269	0
5-storey with BRBs	1	1.278	0	0.771	0.463	0	0
	2	1.188	0.726	0	0	0.516	0
	3	0.767	0	0	0	0	0.807
	4	0.334	0	0.125	0.400	0	0
	5	0.292	0.133	0	0	0.310	0
	6	0.249	0	0.080	0.032	0	0
8-storey seesaw-braced	1	1.722	0	0.585	0.531	0	0
	2	1.297	0.573	0	0	0.559	0
	3	1.040	0	0	0	0	0.771
	4	0.557	0	0.108	0.111	0	0
	5	0.403	0.073	0	0	0.073	0
	6	0.318	0	0	0	0	0.097
8-storey with BRBs	1	2.154	0	0.772	0.683	0	0
	2	2.035	0.749	0	0	0.706	0
	3	1.085	0	0	0	0	0.680
	4	0.404	0	0.180	0.215	0	0
	5	0.341	0.146	0	0	0.177	0
	6	0.300	0	0	0	0	0.079

Table 5
Modal properties of steel structures (soil type D).

Steel structure	Mode number	Period (sec)	Mass participation – Translation x	Mass participation – Translation y	Mass participation – Rocking x	Mass participation – Rocking y	Mass participation – Torsion z
2-storey seesaw-braced	1	0.646	0	0.677	0.268	0	0
	2	0.604	0.641	0	0	0.335	0
	3	0.590	0	0	0	0	0.893
	4	0.283	0.165	0	0	0.591	0
	5	0.281	0	0.095	0.645	0	0
2-storey with BRBs	1	0.571	0	0.749	0.362	0	0
	2	0.543	0.677	0	0	0.441	0
	3	0.480	0	0	0	0	0.814
	4	0.266	0	0.141	0.471	0	0
	5	0.254	0.204	0	0	0.395	0
5-storey seesaw-braced	1	1.520	0	0.677	0.379	0	0
	2	1.335	0.643	0	0	0.437	0
	3	1.023	0	0	0	0	0.899
	4	0.425	0	0.149	0.462	0	0
	5	0.367	0.145	0	0	0.394	0
	6	0.335	0.079	0	0	0.096	0
5-storey with BRBs	1	1.312	0	0.764	0.479	0	0
	2	1.226	0.718	0	0	0.531	0
	3	0.787	0	0	0	0	0.827
	4	0.342	0	0.131	0.400	0	0
	5	0.298	0.141	0	0	0.313	0
	6	0.249	0	0.082	0.035	0	0
8-storey seesaw-braced	1	1.829	0	0.606	0.527	0	0
	2	1.434	0.606	0	0	0.548	0
	3	1.060	0	0	0	0	0.788
	4	0.578	0	0.152	0.165	0	0
	5	0.433	0.219	0	0	0.232	0
	6	0.351	0	0.100	0.041	0	0
8-storey with BRBs	1	2.220	0	0.767	0.695	0	0
	2	2.106	0.744	0	0	0.718	0
	3	1.108	0	0	0	0	0.706
	4	0.410	0	0.178	0.223	0	0
	5	0.347	0.145	0	0	0.184	0
	6	0.311	0	0	0	0	0.110

some sections is greater for the case of soil type D than those of soils B and C. The modal properties, i.e., the periods and the mass participation factors of the first few dominant modes of vibration of the steel structures of Figs. 3 and 4 are shown in Tables 3–5 for the cases of soil types B, C, D, respectively. On the basis of Tables 3–5, one may notice, as it is expected, a period increase of the first modes of the steel structures for the cases of soil types C and D in comparison to soil type B. The mass participation factors for soil types C and D are also different than those of soil type B due to the translation, rocking and torsion of the rigid mat foundation. The seesaw-braced steel structures founded on soil type B are more flexible than the corresponding buckling-restrained braced ones. The modal periods of the 2- and 5-storey steel structures for both bracing types and for soil types C and D are close. However, for soil types C and D, the 8-storey buckling-restrained braced structures are more flexible than the corresponding seesaw-braced ones.

2.4. Ground motions and modelling for inelastic time-history analyses

The steel structures shown in Figs. 3 and 4 are subjected simultaneously to the two horizontal components of the 11 seismic motions presented in Table 6. In this table additional details pertaining to location, date, recording station, moment magnitude M_w and soil type, can also be found. Regarding the soil type, the abbreviations HR, SR and SL correspond to hard rock, sedimentary and conglomerate rock, and soil/alluvium, respectively.

All seismic motions of Table 6 have been obtained from recording instruments located near zones of fault rupture. Near-fault seismic motions have been repeatedly reported in literature to produce major deformation demands and essentially significant residual deformations [37]. It is also known in literature [38] that in the near-fault region, the component of motion normal to the fault is stronger than that parallel to the fault as well as that the fault-normal component exhibits large velocity pulses. Therefore, the fault-normal and fault-parallel components of the seismic motions of Table 6 are maintained without being modified by either amplitude scaling or spectral matching procedures. On the other hand, finding the critical orientation of near-fault seismic motions,

Table 6
Seismic ground motions.

No.	Earthquake, Location	Date	Recording Station	M_w	Soil Type
1.	San Fernando, U.S.A.	February 09, 1971	Pacoima Dam	6.6	HR
2.	Vrancea, Romania	August 30, 1986	INCERC	7.3	SL
3.	Superstition Hills, U.S.A.	November 24, 1987	Parachute Test Site	6.5	SL
4.	Loma Prieta, U.S.A.	October 17, 1989	Los Gatos	7.0	HR
5.	Cape Mendocino, U.S.A.	April 25, 1992	Petrolia	6.9	SR
6.	Landers, U.S.A.	June 28, 1992	Lucerne Valley	7.3	SL
7.	Northridge, U.S.A.	January 17, 1994	Rinaldi Receiving St.	6.7	SL
8.	Northridge, U.S.A.	January 17, 1994	Newhall	6.7	SL
9.	Northridge, U.S.A.	January 17, 1994	Sylmar Converter St.	6.7	SL
10.	Kobe, Japan	January 17, 1995	Takatori	6.9	SL
11.	Christchurch, New Zealand	February 22, 2011	Resthaven	6.3	SL

Table 7
Number of acceptable and unacceptable responses and peak drifts of steel structures without SSI (fixed base).

Steel structure	Seismic incident angle	Unacceptable response - Number of motions	Acceptable response - Number of motions	Acceptable response - Peak IDR (%)	Acceptable response - Peak RIDR (%)
2-storey seesaw-braced	0°	1	10	1.50	0.21
	90°	0	11	1.50	0.16
	180°	1	10	1.50	0.23
2-storey with BRBs	0°	0	11	4.00	0.24
	90°	0	11	3.20	0.27
	180°	4	7	2.50	0.24
5-storey seesaw-braced	**0°**	4	7	3.00	0.55
	90°	6	5	2.60	0.27
	180°	4	7	1.80	0.27
5-storey with BRBs	0°	5	6	3.80	0.24
	90°	5	6	3.60	0.48
	180°	5	6	2.60	0.17
8-storey seesaw-braced	0°	8	3	1.50	0.30
	90°	8	3	2.40	0.45
	180°	8	3	1.40	0.28
8-storey with BRBs	0°	4	7	3.00	0.20
	90°	5	6	3.40	0.31
	180°	8	3	3.00	0.12

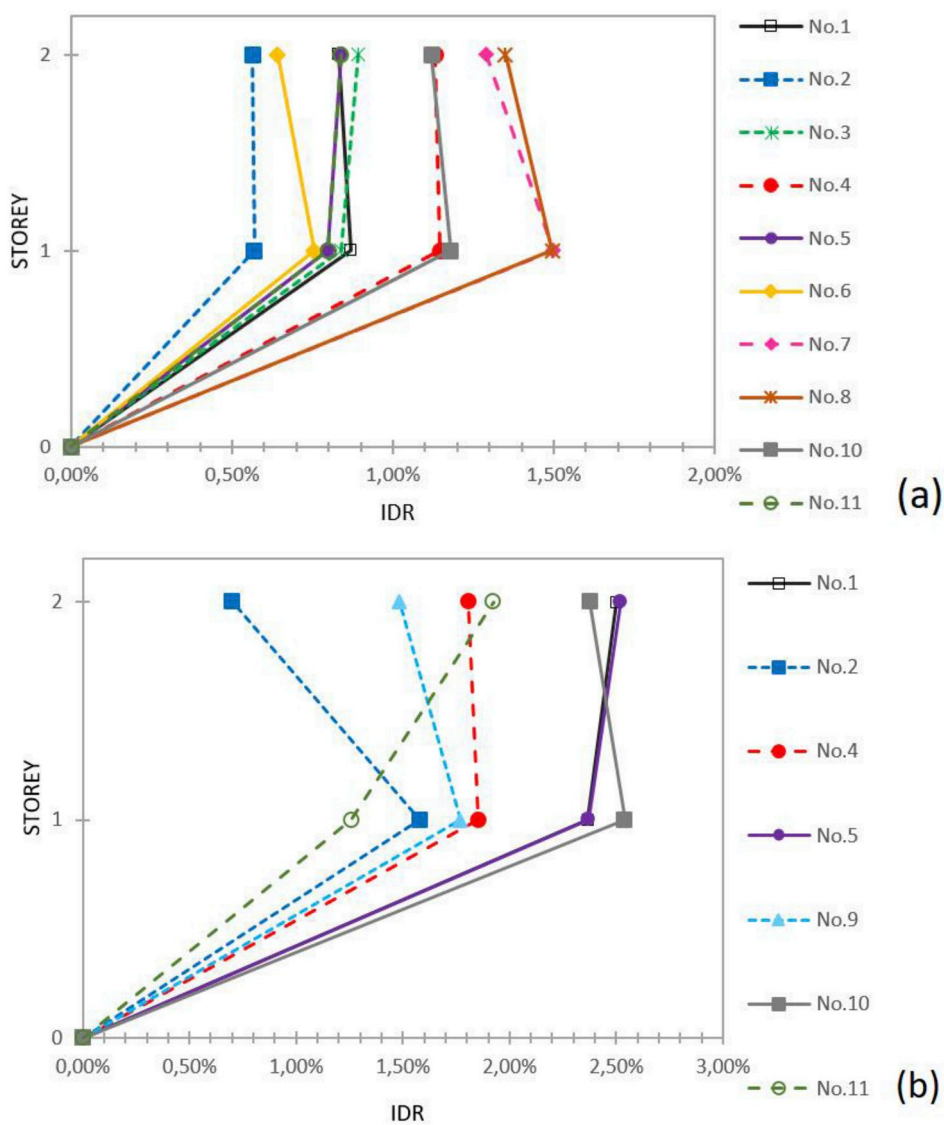

Fig. 5. IDR responses of the 2-storey seesaw-braced (a) and buckling-restrained braced (b) fixed base steel structures.

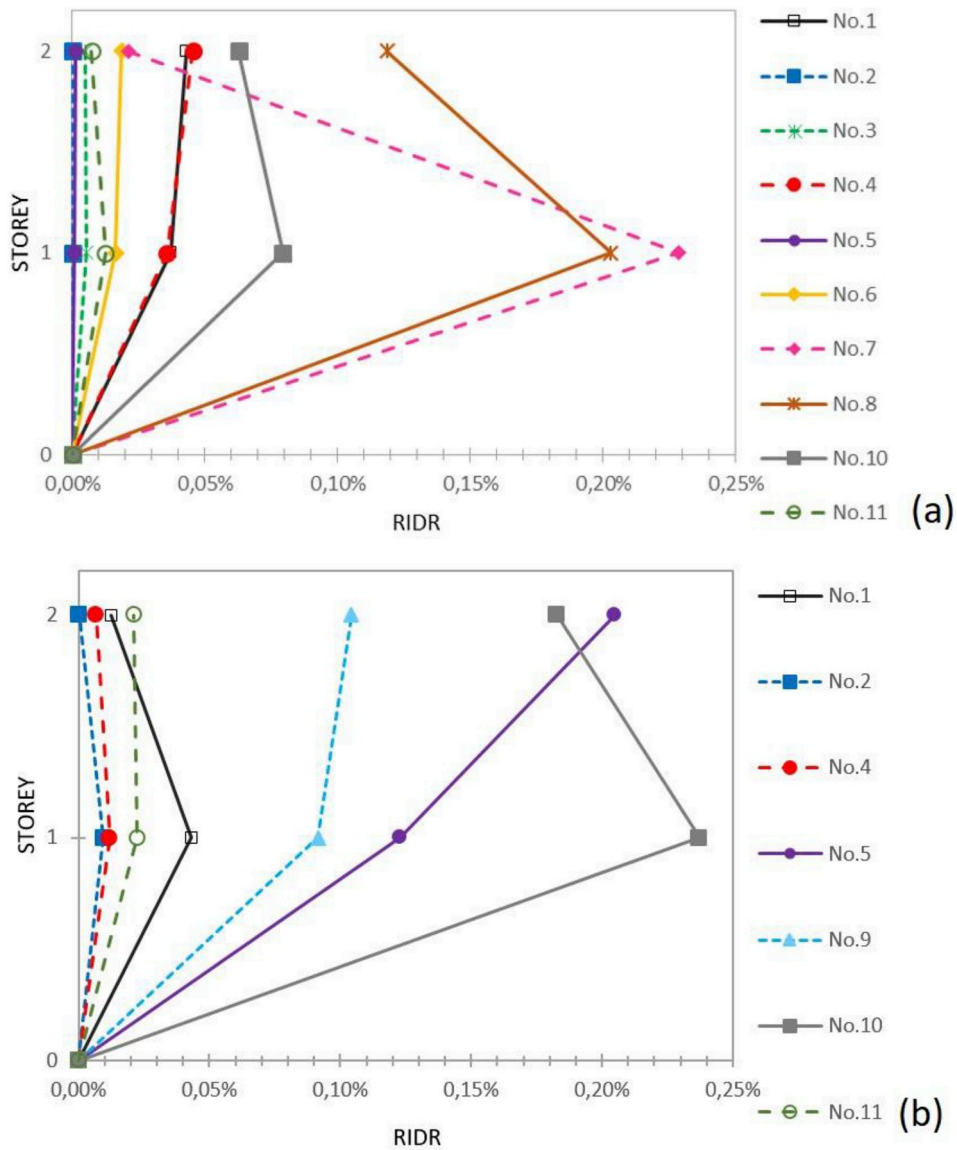

Fig. 6. RIDR responses of the 2-storey seesaw-braced (a) and buckling-restrained braced (b) fixed base steel structures.

i.e., the one that produces the maximum seismic response, is also a challenging task since this critical orientation varies not only with the seismic motion pair considered but also with the response parameter of interest (IDR or RIDR) [39–41]. In view of the above, the seismic motions of Table 6 are employed in time-history seismic analyses according to their as-recorded orientation. More specifically, these seismic motions are applied in the direction of the two orthogonal structural axes of Fig. 1 considering three values for the horizontal angle of seismic incidence, i.e., 0°, 90° and 180°, with respect to the geometric centre of the framing system of Fig. 1.

Large levels of inelastic seismic response are expected when the steel structures of Figs. 3 and 4 are subjected to the seismic motions of Table 6. In particular, the mean 5%-damped elastic response spectrum of the seismic motions of Table 6 in each direction surpasses the elastic design spectrum (mentioned previously in section 2) by at least 10% for a period range $0.2T_1$-$2.0T_1$, where T_1 is the fundamental period of the structure under study. The lower and upper bounds on T_1 are selected to capture higher mode response and period elongation effects, respectively.

The seismic response of the steel structures shown in Figs. 3 and 4 is determined through inelastic time-history analyses using SAP [32] for the seesaw-braced structures and ETABS [34] for the buckling-restrained braced ones. Geometrical non-linearities are also taken into account. Beams and columns are modelled using standard frame elements with concentrated plasticity and 2% strain hardening. Plastic hinges in beams are formed due to uniaxial bending, whereas those in columns due to interaction of axial force-biaxial bending. The limits for plastic hinge rotations for the frame members are defined in Refs. [32,34] according to ASCE 41-17 [38]. The innate viscous damping of the steel structure is considered to be 3%. The constants of the Rayleigh damping matrix are then defined utilizing the fundamental period of the structure and the period of its highest mode of significance. Diaphragm action is assumed at every floor due to the presence of the composite slab.

The hysteresis model of the BRBs should include an appropriate isotropic hardening law or a combination of isotropic and kinematic hardening [8,42,43]. This is particularly important when assessing the force demands imposed to beams and columns by the BRBs. However, in an effort to stay on the conservative side, in the seismic response computations conducted in this work, the BRB is modelled as an inelastic

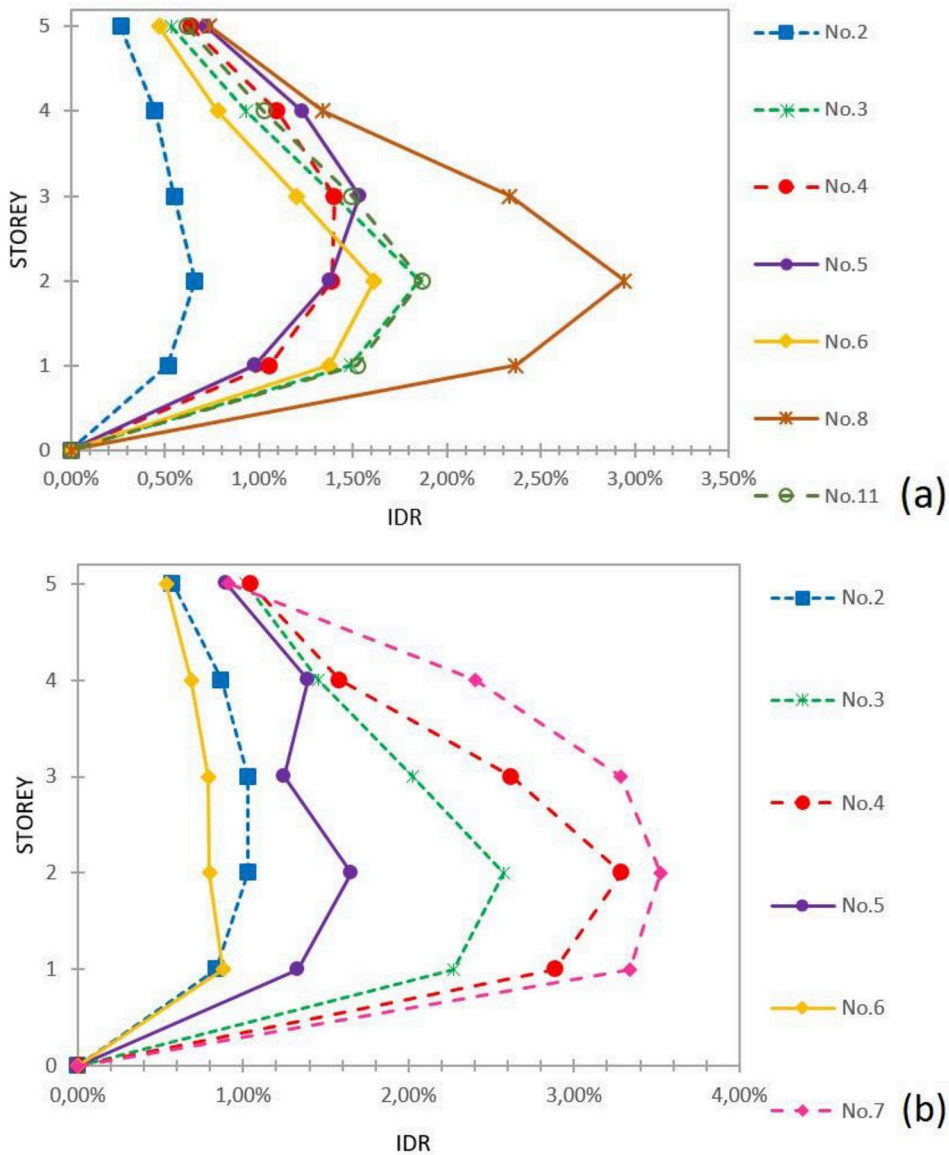

Fig. 7. IDR responses of the 5-storey seesaw-braced (a) and buckling-restrained braced (b) fixed base steel structures.

truss member on the basis of an equivalent area [19,33]. The post-yield stiffness of the BRB is assumed to be 2% of its axial elastic stiffness. A nominal yield strength of 245 MPa is assumed for the BRB in order to acknowledge the variability of yield stress in the material of the core. The gusset plate connections of the BRB-to-beam and of the BRB-to-column are not modelled, even though they may affect the effectiveness of the BRBs, since such details would introduce a number of additional parameters the investigation of which is beyond the scope of this work.

Linear viscous dampers are modelled as discrete damping elements using the 'Link element' option implemented in Refs. [32,34]. The horizontal and vertical steel plates of the seesaw are modelled as rigid elements, whereas the spiral strand ropes are modelled as cable elements considering geometrical non-linearities and pretension. Depending on the length and properties of the spiral strand ropes, the level of pre-tension is different for each steel structure, e.g., approximately 16 kN for the 2-storey one. Nevertheless, this pretension is necessary because it ensures direct activation of the spiral strand ropes under the initiation and the subsequent reversals of seismic motion.

The 'Link element' of Refs [32,34] is also employed to model the discrete system of springs, dashpots and masses [35] in order to capture the effects of SSI. The inelastic time-history seismic analyses are firstly conducted for fixed base steel structures where SSI is absent, and then for steel structures founded on soil types C or D where SSI is present.

3. Seismic response results

In the following, the drift responses of seesaw-braced and buckling-restrained braced steel structures of Figs. 3 and 4 are compared on the basis of similar seismic input data (seismic motions, angle of seismic incidence, soil type). In particular, height wise distributions for peak IDRs and RIDRs as well as the seismic motions for which acceptable seismic response occurs are provided. Unacceptable seismic response is attested if one or more of the following conditions are met: a) the spiral strand ropes of the seesaw-braced structures fail; b) the axial displacement of the BRBs surpasses its design value; c) RIDRs are in excess of 0.55%; d) the axial compression in columns of the lowest story is beyond 60% of their design axial strength; e) hinge rotations in beams and columns are beyond the life-safety level (LS) [32,34,38]; f) plastic hinges occur at both ends of columns and the formation of a soft-storey

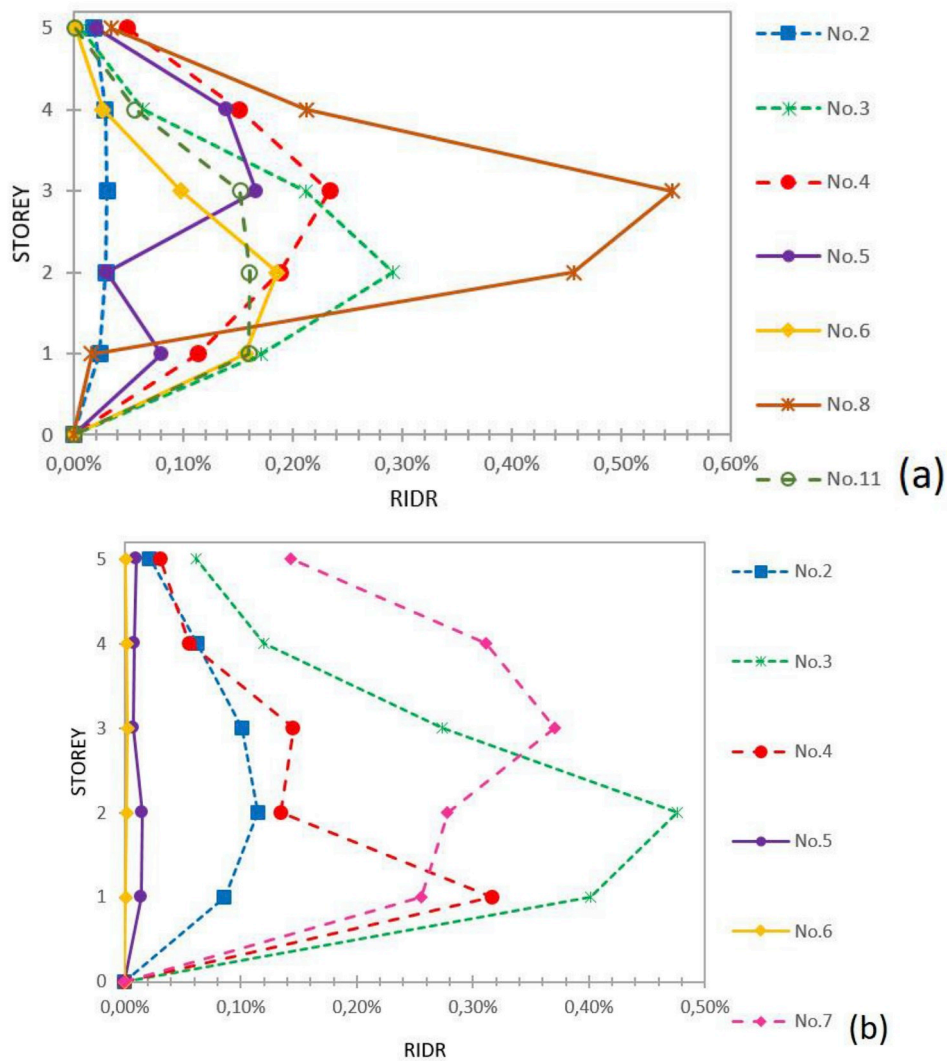

Fig. 8. RIDR responses of the 5-storey seesaw-braced (a) and buckling-restrained braced (b) fixed base steel structures.

mechanism starts. Overall, if an unacceptable seismic response is found, this indicates a high probability of collapse of the particular steel structure under consideration.

Regarding the behavior of the seesaw-braced steel structures, in all analyses performed, the linear viscous dampers do not fail, i.e., their maximum stroke or maximum force is not exceeded. On the other hand, for a significant number of seismic analyses either the value of 0.55% for RIDR is exceeded and/or the design tensile strength of the spiral strand ropes is exceeded. The IDR and RIDR results of these seismic analyses are not included in the corresponding plots in order to reveal the cases (number of seismic motions) in which the seesaw-braced steel structures experience unacceptable seismic response. Excluding, thus, those seismic analyses where spiral strand ropes fail and/or RIDR exceeds 0.55%, one observes the following for the rest seismic analyses: i) plastic hinge rotations of beams and columns are found to be either below the IO (Immediate Occupancy) level or between the IO and LS (Life Safety) levels, while the LS level is never exceeded and ii) soft-storey mechanisms do not occur.

Referring to the behavior of the buckling-restrained braced steel structures, in all analyses performed, the design axial displacement of the BRBs is not exceeded. Nevertheless, for a significant number of seismic analyses, undesired plastic hinge excursions take place at the upper end of the columns of the lowest storeys, leading, thus, to a soft-storey mechanism. This is mainly attributed to the simultaneous yield of a number of BRBs. A similar observation has also been reported in Ref. [44]. The IDR and RIDR results of these seismic analyses are not included in the corresponding plots in order to reveal the cases (number of seismic motions) in which the buckling-restrained braced steel structures experience unacceptable seismic response. Excluding, thus, those seismic analyses where soft-storey mechanism occurs, one observes the following for the rest of seismic analyses: i) plastic hinge rotations of beams and columns are found to be either below the IO (Immediate Occupancy) level or between the IO and LS (Life Safety) levels, while the LS level is never exceeded.

The legends in the figures involving IDR and RIDR plots correspond to the numbering (No.) of seismic motions following Table 6. For the cases of steel structures founded on soil types C and D, the net IDR and RIDR values in the direction of the two orthogonal structural axes of Fig. 1 are computed. More specifically, the relative displacement $\Delta\delta_i$ of the ith storey is calculated as: $\Delta\delta_i = \Delta_i - \Delta_{i-1} - \theta H$, where Δ_i and Δ_{i-1} are the displacement of the ith and $(i-1)^{th}$ storey, respectively, θ is the rotation of the foundation in the direction considered and H is the height of the ith storey.

3.1. Steel structures neglecting SSI (fixed base condition)

The number of acceptable and unacceptable responses as well as the peak IDR and RIDR values of the acceptable responses neglecting SSI,

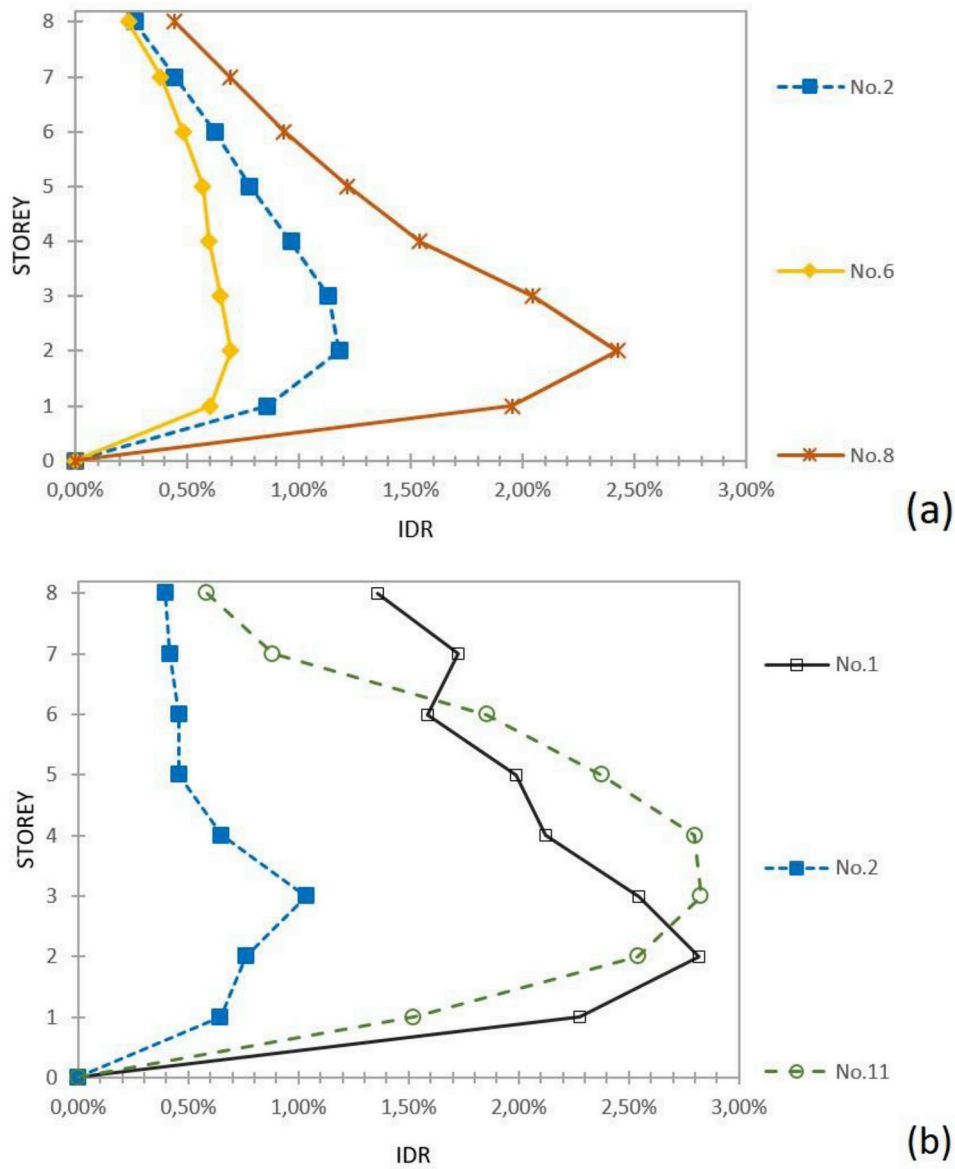

Fig. 9. IDR responses of the 8-storey seesaw-braced (a) and buckling-restrained braced (b) fixed base steel structures.

are shown in Table 7 where the following observations can be made: a) the 2-storey seesaw-braced steel structures perform slightly better than those equipped with buckling-restrained braces, in terms of the number of unacceptable responses (2 against 4) and peak RIDR (0.23% against 0.27%); b) the 5-storey seesaw-braced steel structures perform marginally better than the buckling-restrained braced ones in terms of the number of unacceptable responses (14 against 15) but exhibit larger peak RIDR (0.55% against 0.48%); c) the 8-storey seesaw-braced steel structures perform worse than the buckling-restrained braced ones in terms of the number of unacceptable responses (24 against 17) and exhibit larger peak RIDR (0.45% against 0.31%). Figs. 5–10 provide the comparative peak IDR and RIDR responses of the steel structures subjected to the seismic motions of Table 6 for the most unfavourable (on the basis of the number of unacceptable responses and/or peak acceptable RIDR) case of seismic incident angle (marked with bold characters in Table 7). RIDR values of the unacceptable responses reach 1.2% for both seesaw-braced and buckling-restrained braced steel structures fixed at their base.

3.2. *Steel structures considering SSI – soil type C*

The number of acceptable and unacceptable responses as well as the peak IDR and RIDR values of the acceptable responses considering SSI, are shown in Table 8 where the following observations can be made: a) the 2-storey seesaw-braced steel structures perform slightly worse than the buckling-restrained braced ones in terms of the number of unacceptable responses (4 against 3) and peak RIDR (0.42% against 0.32%); b) the 5-storey seesaw-braced steel structures perform worse than the buckling-restrained braced ones in terms of the number of unacceptable responses (20 against 10) and peak RIDR (0.47% against 0.38%); c) the 8-storey seesaw-braced steel structures perform better than the buckling-restrained braced ones in terms of the number of unacceptable responses (15 against 19), however, they exhibit the same peak RIDR (0.45%). Figs. 11–16 provide the comparative peak IDR and RIDR responses of the steel structures subjected to the seismic motions of Table 6 for the most unfavourable (on the basis of the number of unacceptable responses and/or peak acceptable RIDR) case of seismic incident angle (marked with bold characters in Table 8). RIDR values of the

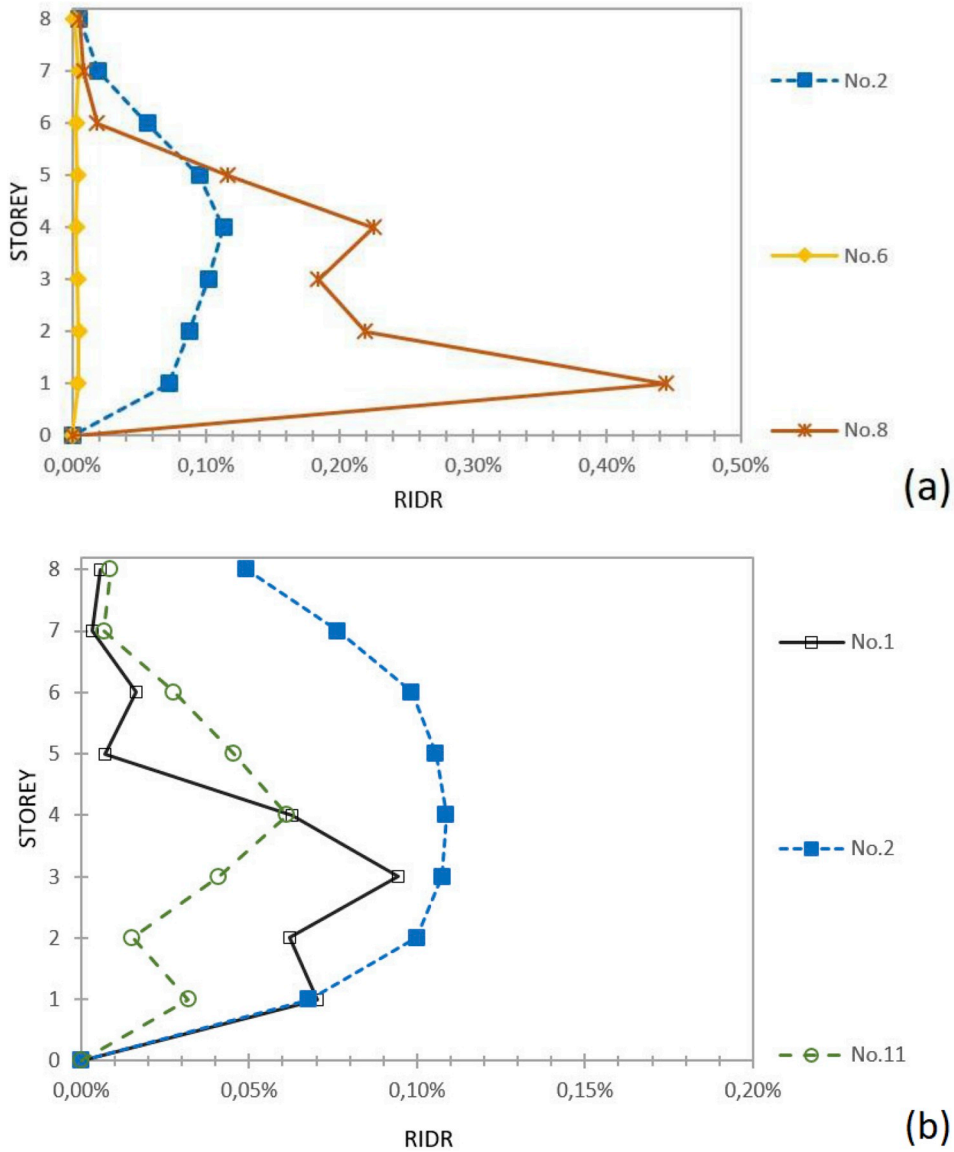

Fig. 10. RIDR responses of the 8-storey seesaw-braced (a) and buckling-restrained braced (b) fixed base steel structures.

Table 8
Number of acceptable and unacceptable responses and peak drifts of steel structures with SSI (soil type C).

Steel structure	Seismic incident angle	Unacceptable response - Number of motions	Acceptable response - Number of motions	Acceptable response - Peak IDR (%)	Acceptable response - Peak RIDR (%)
2-storey seesaw-braced	**0**°	2	9	3.20	0.36
	90°	0	11	2.70	0.30
	180°	2	9	3.20	0.42
2-storey with BRBs	0°	0	11	4.20	0.25
	90°	1	10	4.00	0.22
	180°	2	9	3.60	0.32
5-storey seesaw-braced	0°	7	4	2.40	0.33
	90°	7	4	3.10	0.47
	180°	6	5	2.20	0.33
5-storey with BRBs	0°	2	9	5.00	0.37
	90°	3	8	4.20	0.38
	180°	4	7	3.70	0.25
8-storey seesaw-braced	0°	4	7	2.70	0.32
	90°	7	4	3.20	0.33
	180°	4	7	2.80	0.45
8-storey with BRBs	0°	6	5	2.70	0.25
	90°	6	5	2.60	0.45
	180°	7	4	2.70	0.20

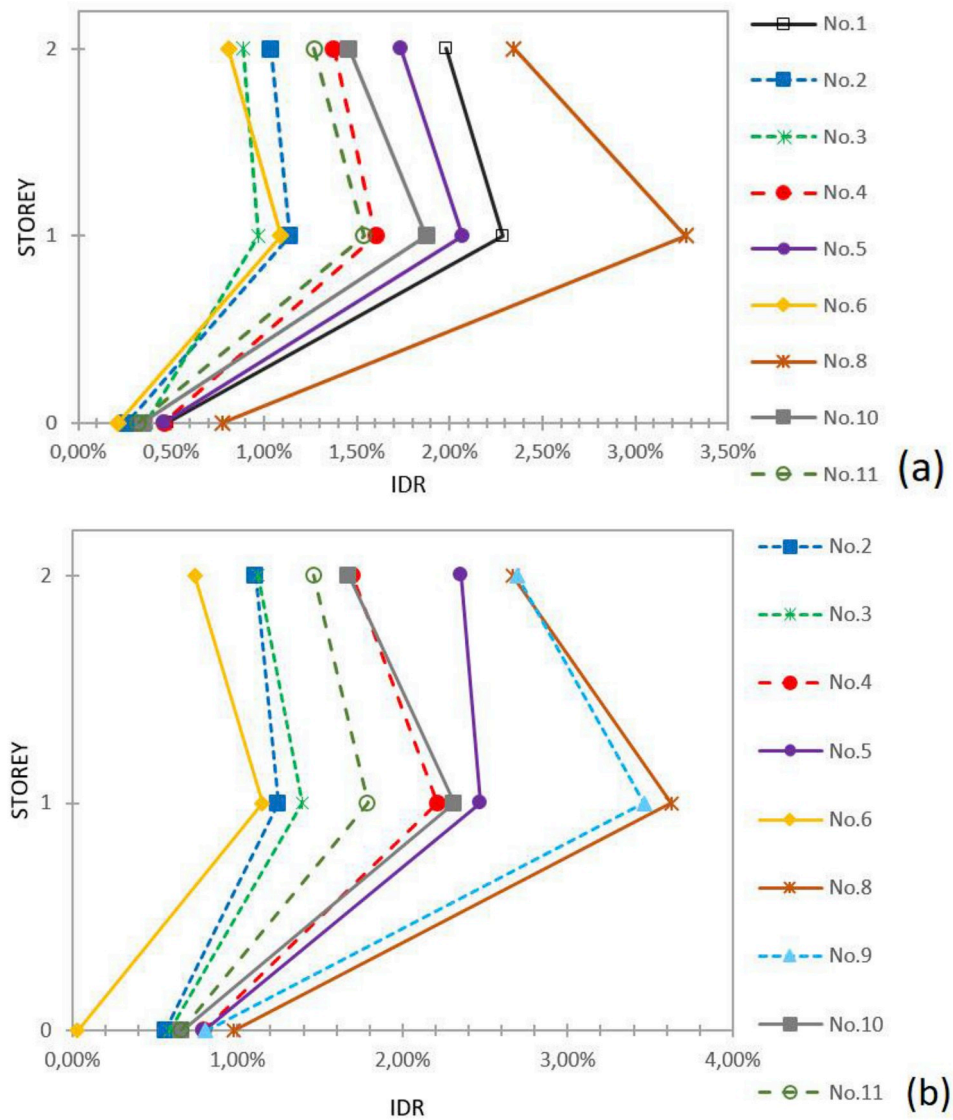

Fig. 11. IDR responses of the 2-storey seesaw-braced (a) and buckling-restrained braced (b) steel structures (soil type C).

unacceptable responses reach 1.5% for both seesaw-braced and buckling-restrained braced steel structures.

3.3. Steel structures considering SSI – soil type D

The number of acceptable and unacceptable responses as well as the peak IDR and RIDR values of the acceptable responses considering SSI, are shown in Table 9. Based on these results the following observations can be made: a) the 2-storey seesaw-braced steel structures perform slightly better than the buckling-restrained braced ones in terms of the number of unacceptable responses (5 against 7), but they exhibit larger peak RIDR (0.43% against 0.39%); b) the 5-storey seesaw-braced steel structures perform worse than the buckling-restrained braced ones in terms of the number of unacceptable responses (24 against 9) and peak RIDR (0.50% against 0.26%); c) the 8-storey seesaw-braced steel structures perform slightly better than the buckling-restrained braced ones in terms of the number of unacceptable responses (15 against 17), however, they exhibit larger peak RIDR (0.51 against 0.27%). Figs. 17–22 provide the comparative peak IDR and RIDR responses of the steel structures subjected to the seismic motions of Table 6 for the most unfavourable (on the basis of the number of unacceptable responses and/or peak acceptable RIDR) case of seismic incident angle (marked with bold characters in Table 9). RIDR values of the unacceptable responses reach 1.6% for both seesaw-braced and buckling-restrained braced steel structures.

3.4. Discussion on the drift response results

It is of interest to compare the drift response results obtained from inelastic time-history seismic analyses per type of structure, taking into account the effects of SSI and angle of seismic incidence. In total, 99 cases involving 11 seismic motions, 3 angles of seismic incidence and 3 base conditions (fixed base, base founded on soil types C and D) are studied for each one of the structures of Figs. 3 and 4.

Starting with the 2-storey steel structures, a small advantage is given to the seesaw-braced structures over the buckling-restrained braced ones in terms of total acceptable responses regardless of the presence or absence of SSI and the angle of seismic incidence. In particular, seesaw-braced structures provide acceptable responses in 88 cases in contrast to 85 cases for the buckling-restrained braced structures. However, one should note that when SSI effects are included, the seesaw-braced structures exhibit larger peak RIDR in comparison to the buckling-

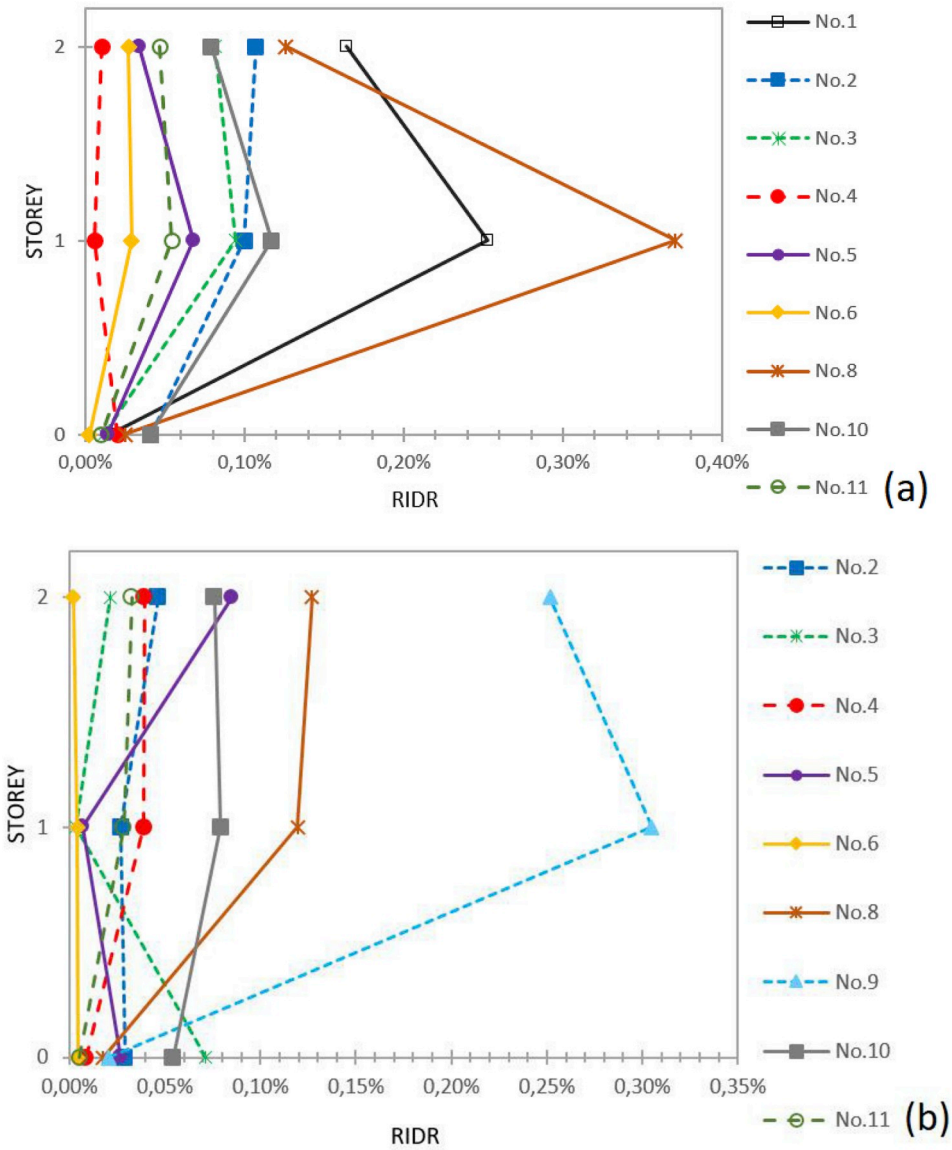

Fig. 12. RIDR responses of the 2-storey seesaw-braced (a) and buckling-restrained braced (b) steel structures (soil type C).

restrained braced ones. The RIDR trend is reversed when SSI is absent. For the two types of braced structures studied in this work, peak IDRs are different even though a similar drift concentration along height is exhibited.

Moving to the 5-storey steel structures, major advantage is given to the buckling-restrained braced structures over the seesaw-braced ones in terms of total acceptable responses in presence of SSI and regardless of the angle of seismic incidence. Out of the 66 (SSI considered) cases, buckling-restrained braced structures provide acceptable response in 48 in contrast to just 22 of the seesaw-braced structures. On the other hand, when SSI is absent, out of 33 cases, the seesaw-braced structures provide acceptable response in 19 and the buckling-restrained braced structures in 20. Considering or neglecting SSI, seesaw-braced structures exhibit larger peak RIDRs in comparison to buckling-restrained braced ones. The two types of structures studied in this work exhibit different peak IDRs but similar drift concentration patterns along height.

Finally, regarding the 8-storey steel structures, advantage is given to the seesaw-braced ones over the buckling-restrained braced ones in terms of total acceptable responses in presence of SSI and regardless of the angle of seismic incidence. Out of the 66 (SSI considered) cases, seesaw-braced structures provide acceptable response in 36 in contrast to 30 of the buckling-restrained braced structures. The trend is reversed when SSI is absent where out of 33 cases, the buckling-restrained braced structures provide acceptable response in 16 and the seesaw-braced structures in 9. Considering or neglecting SSI, seesaw-braced structures exhibit larger peak RIDRs in comparison to buckling-restrained braced ones. Nevertheless, one should note that for soil type C, both types of braced structures exhibit the same peak RIDR. Peak IDRs and drift concentration patterns along the height are different for the two types of braced structures.

4. Synopsis and conclusions

The seismic drift responses of some low-rise 3D seesaw-braced and buckling-restrained braced steel structures are numerically investigated and the results are discussed from a comparative point of view. The numerical investigation involves a number of seismic motions and seismic incident angles as well as the presence or absence of SSI.

The comparative seismic drift response results demonstrate that seesaw-braced and buckling-restrained braced steel structures exhibit

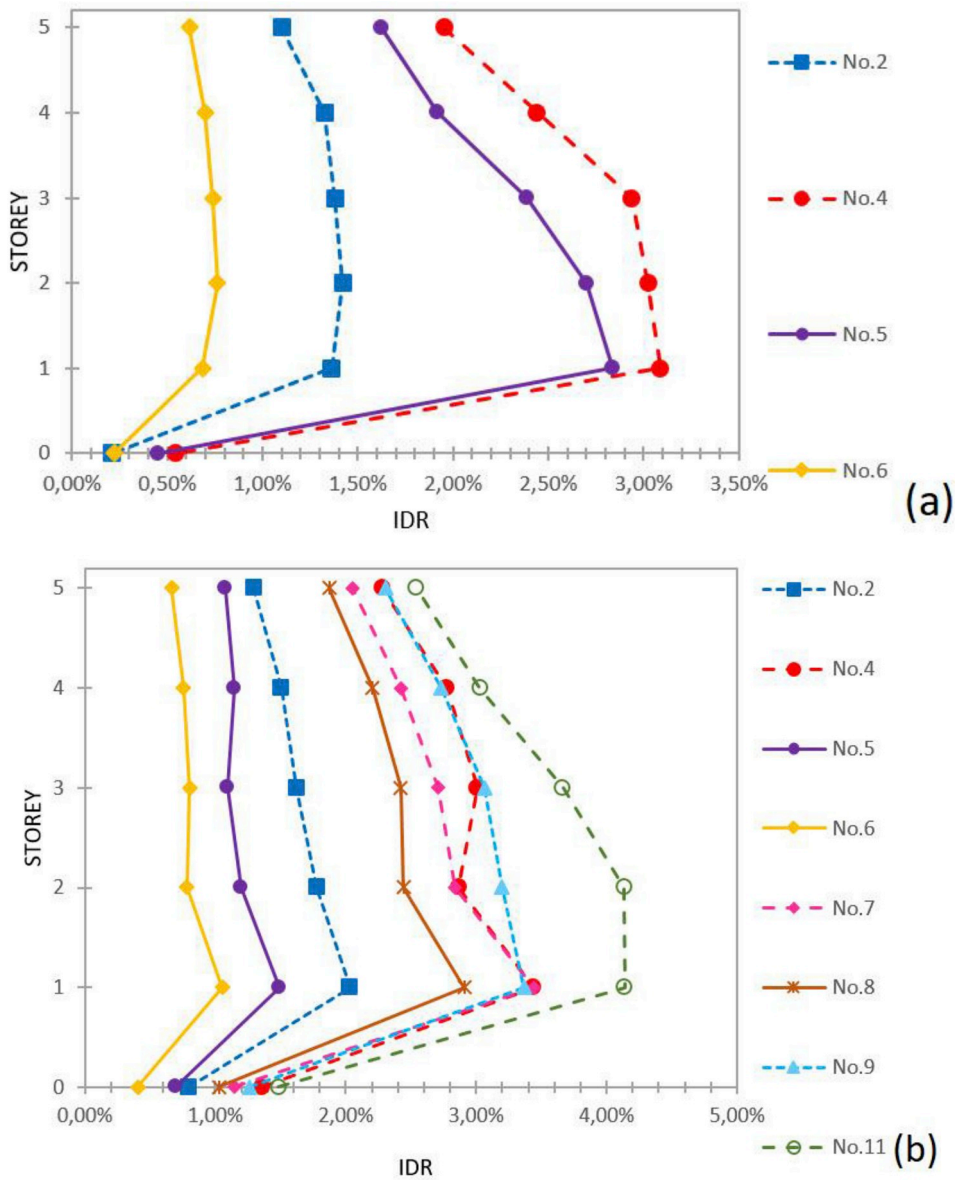

Fig. 13. IDR responses of the 5-storey seesaw-braced (a) and buckling-restrained braced (b) steel structures (soil type C).

different peak IDR values but in many cases similar drift concentrations, i.e., drift accumulation at specific storeys. Peak RIDR should be the decisive seismic design factor for these two types of braced steel structures. However, in particular, this study reveals that larger peak RIDRs can be observed for the seesaw-braced steel structures than those outfitted with buckling-restrained braces. Nevertheless, it should be noted that the comparative drift response results between these two types of braced steel structures depend on the orientation (layout) of the columns as well as on the position and configuration of the braces. Therefore, the seismic drift results presented herein are only indicative of the seesaw-braced and buckling-restrained braced structures studied, but certainly offer a clue towards the overall seismic behavior of these special types of braced steel structures.

It is important, as a future work, to conduct seismic analyses of these two types of braced steel structures for different column layouts and brace configurations as well as for specific levels of expected seismic motion, i.e., corresponding to operational, design basis and maximum credible earthquake. Incremental dynamic analyses should be also performed in order to assess the collapse resistance of these two types of braced steel structures. To further investigate the seismic damage and collapse potential of these two types of braced steel structures, a more detail modelling using finite elements is required for gusset plates (buckling, fracture of welds), BRB (out-of-plane buckling, fracture) and spiral strand ropes (anchorage to gusset plates, localized bending close to anchorage points).

The seismic behavior of steel structures with BRBs constitutes mature knowledge that has been already implemented in seismic design codes. On the contrary, knowledge of the seismic behavior of steel structures equipped with the seesaw system is still limited. The purpose of this work is to offer some evidence towards the approval or disapproval of the seesaw-braced steel structures from the engineering community. Control of RIDR, the 'Achilles heel', for seesaw-braced and buckling-restrained braced steel structures is a 'challenge' for the former but a 'must' for the latter.

Declaration of competing interest

We have no conflict of interest to declare.

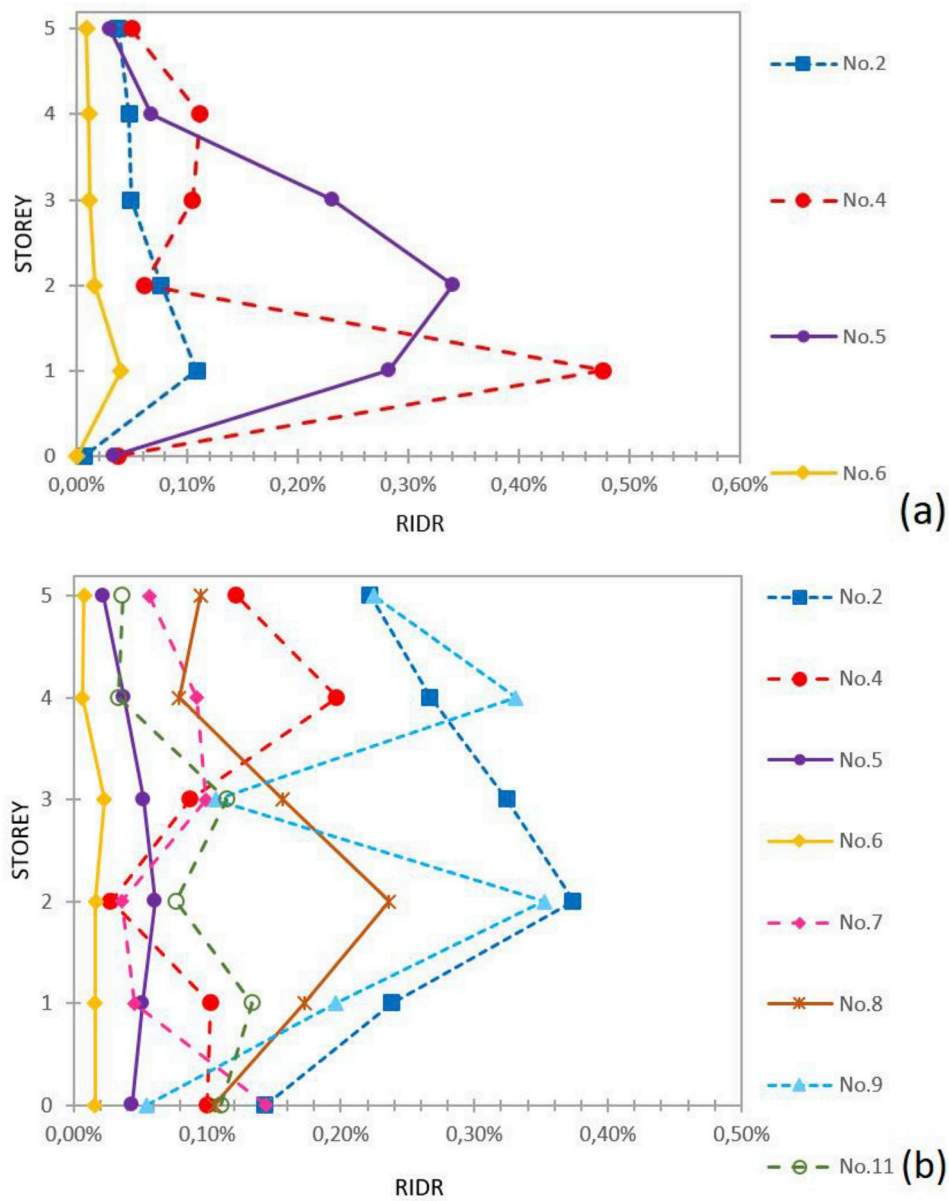

Fig. 14. RIDR responses of the 5-storey seesaw-braced (a) and buckling-restrained braced (b) steel structures (soil type C).

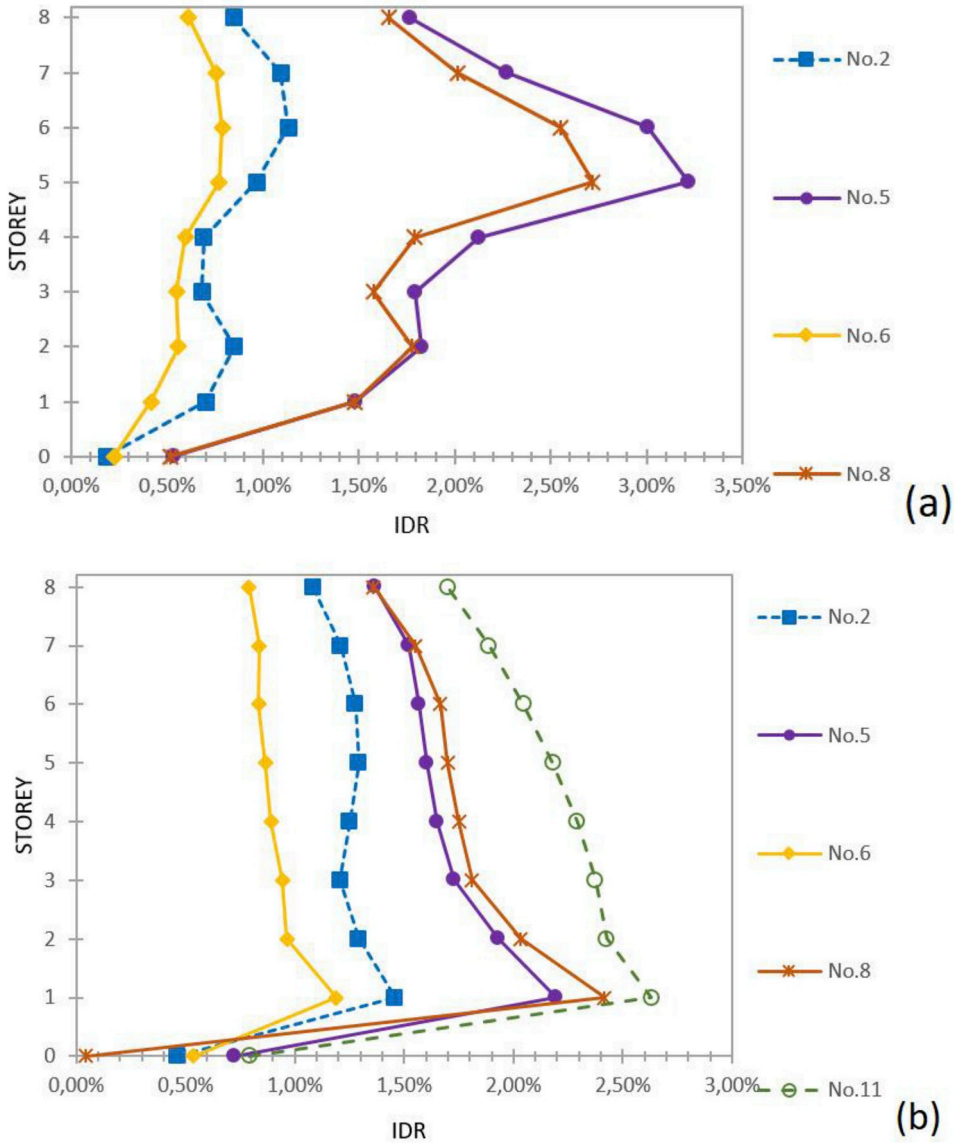

Fig. 15. IDR responses of the 8-storey seesaw-braced (a) and buckling-restrained braced (b) steel structures (soil type C).

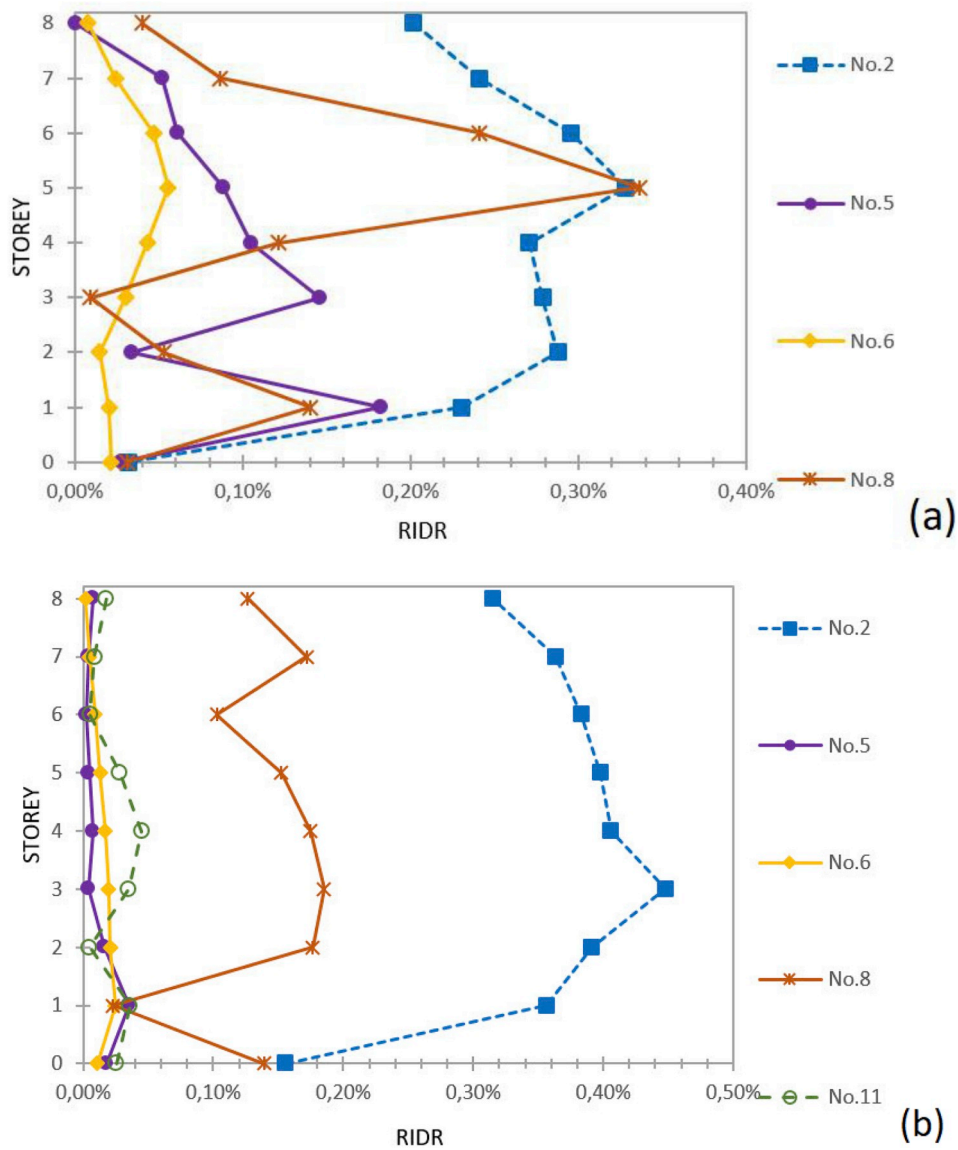

Fig. 16. RIDR responses of the 8-storey seesaw-braced (a) and buckling-restrained braced (b) steel structures (soil type C).

Table 9
Number of acceptable and unacceptable responses and peak drifts of steel structures with SSI (soil type D).

Steel structure	Seismic incident angle	Unacceptable response - Number of motions	Acceptable response - Number of motions	Acceptable response - Peak IDR (%)	Acceptable response - Peak RIDR (%)
2-storey seesaw-braced	**0**°	2	9	3.50	0.43
	90°	0	11	2.90	0.37
	180°	3	8	2.30	0.33
2-storey with BRBs	**0**°	3	8	4.90	0.23
	90°	2	9	5.00	0.17
	180°	2	9	5.00	0.39
5-storey seesaw-braced	0°	8	3	2.30	0.15
	90°	8	3	3.10	0.50
	180°	8	3	2.30	0.12
5-storey with BRBs	0°	2	9	5.00	0.26
	90°	3	8	4.50	0.26
	180°	4	7	3.60	0.15
8-storey seesaw-braced	**0**°	4	7	3.00	0.27
	90°	8	3	2.00	0.14
	180°	3	8	3.10	0.51
8-storey with BRBs	0°	6	5	2.70	0.24
	90°	5	6	2.90	0.27
	180°	6	5	2.70	0.18

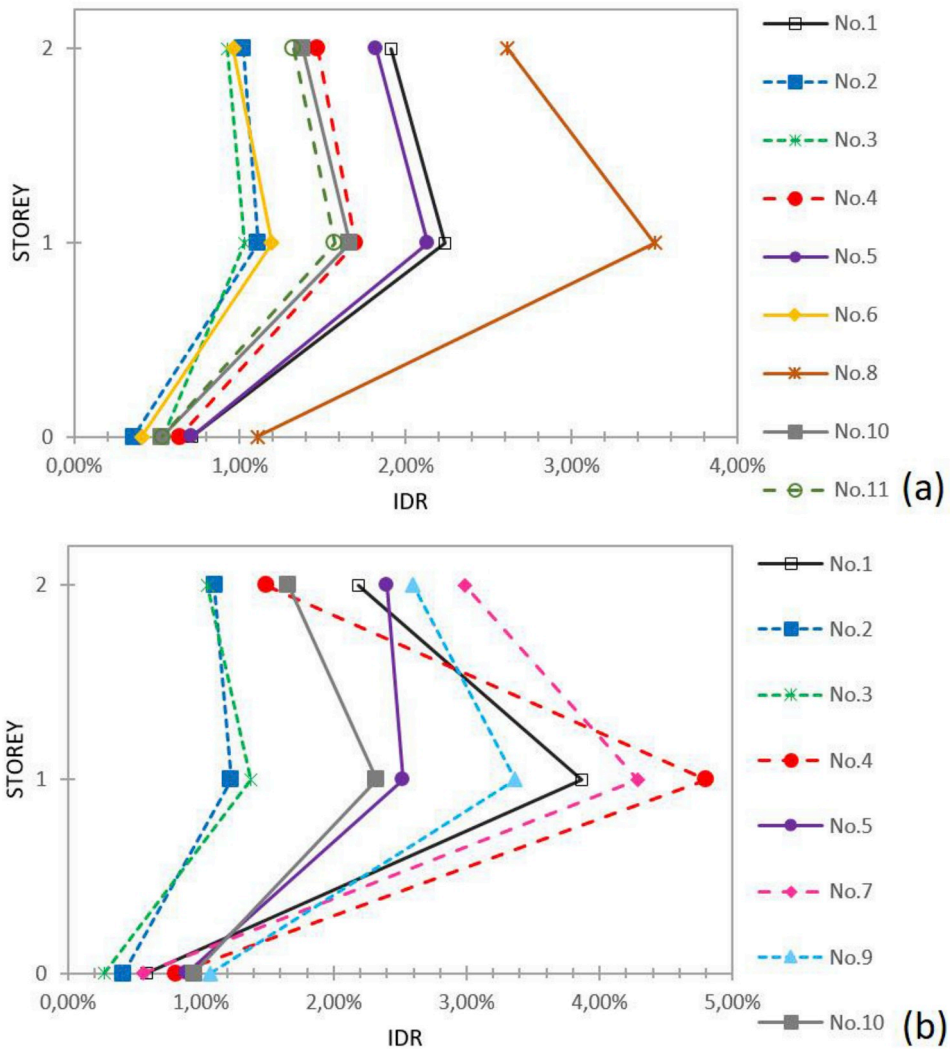

Fig. 17. IDR responses of the 2-storey seesaw-braced (a) and buckling-restrained braced (b) steel structures (soil type D).

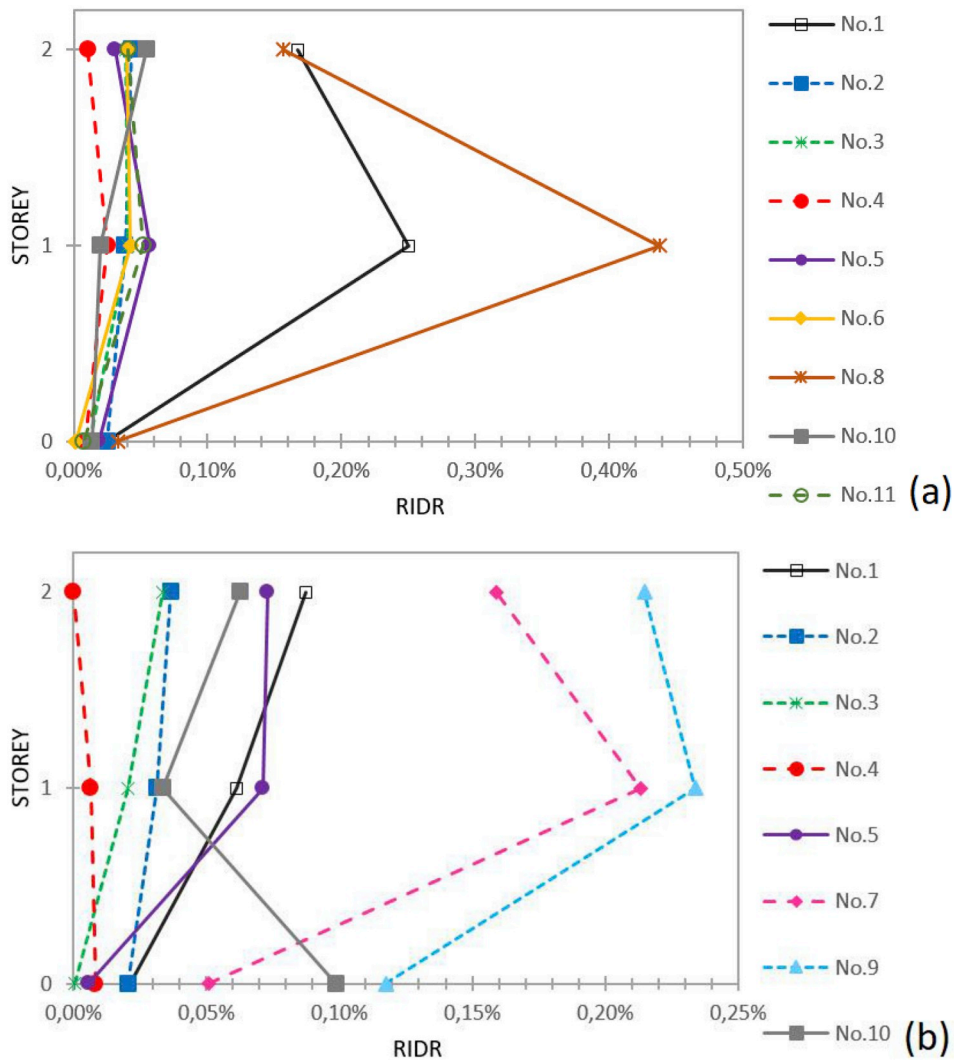

Fig. 18. RIDR responses of the 2-storey seesaw-braced (a) and buckling-restrained braced (b) steel structures (soil type D).

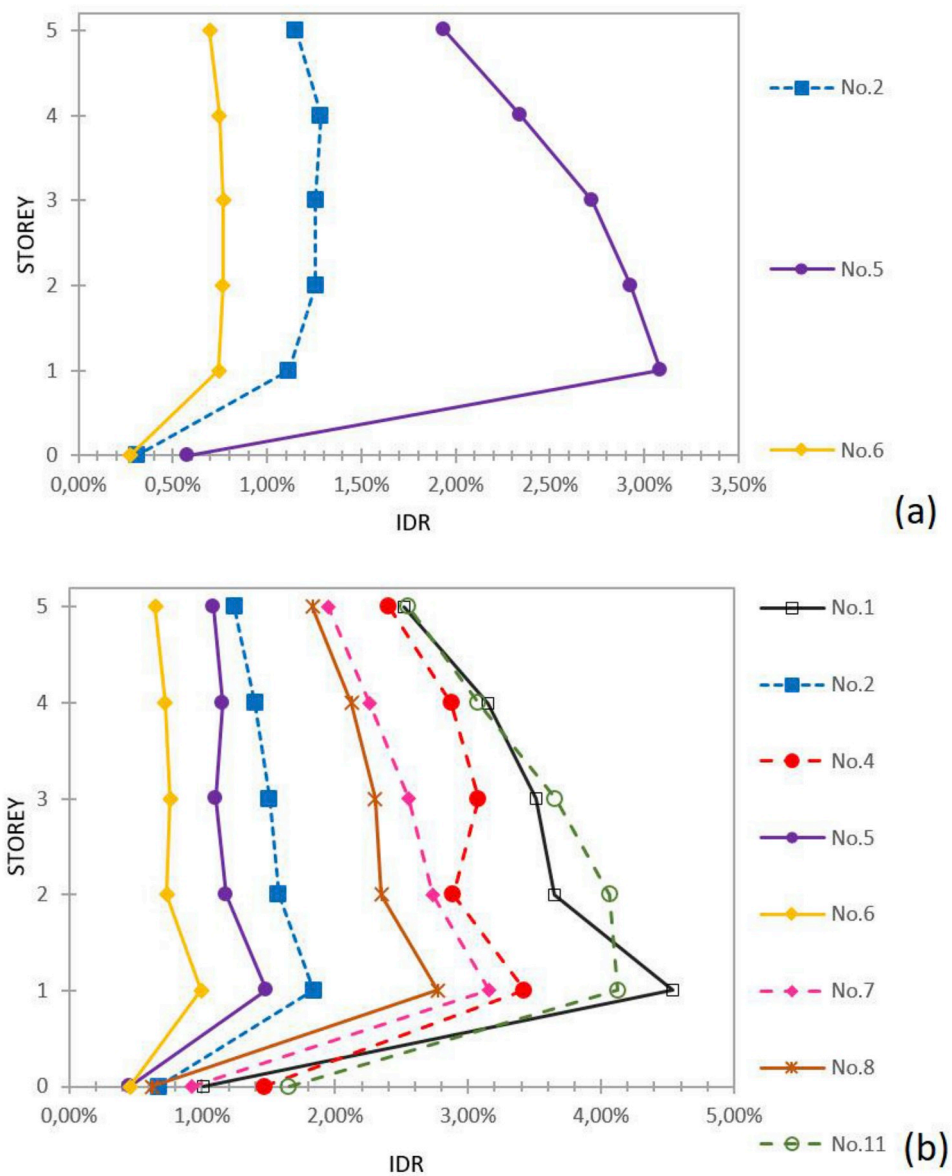

Fig. 19. IDR responses of the 5-storey seesaw-braced (a) and buckling-restrained braced (b) steel structures (soil type D).

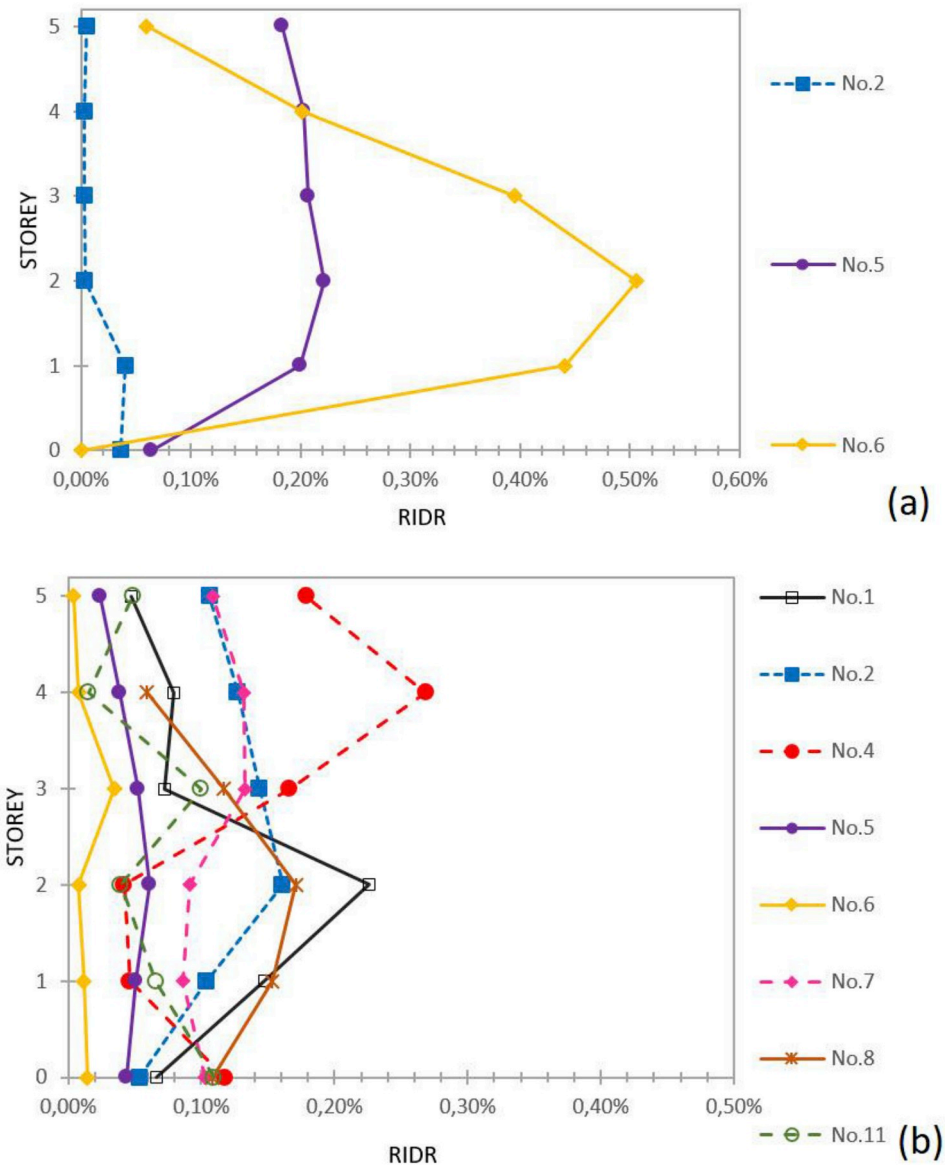

Fig. 20. RIDR responses of the 5-storey seesaw-braced (a) and buckling-restrained braced (b) steel structures (soil type D).

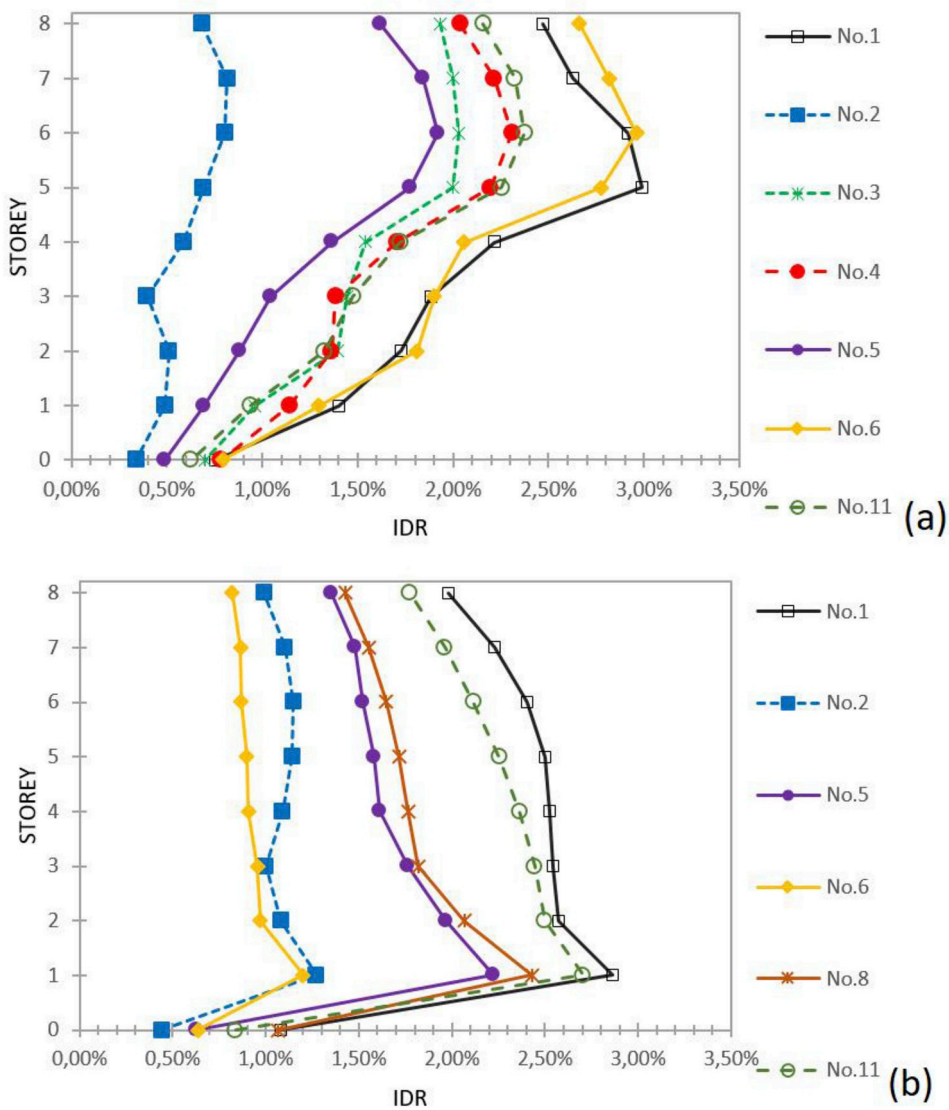

Fig. 21. IDR responses of the 8-storey seesaw-braced (a) and buckling-restrained braced (b) steel structures (soil type D).

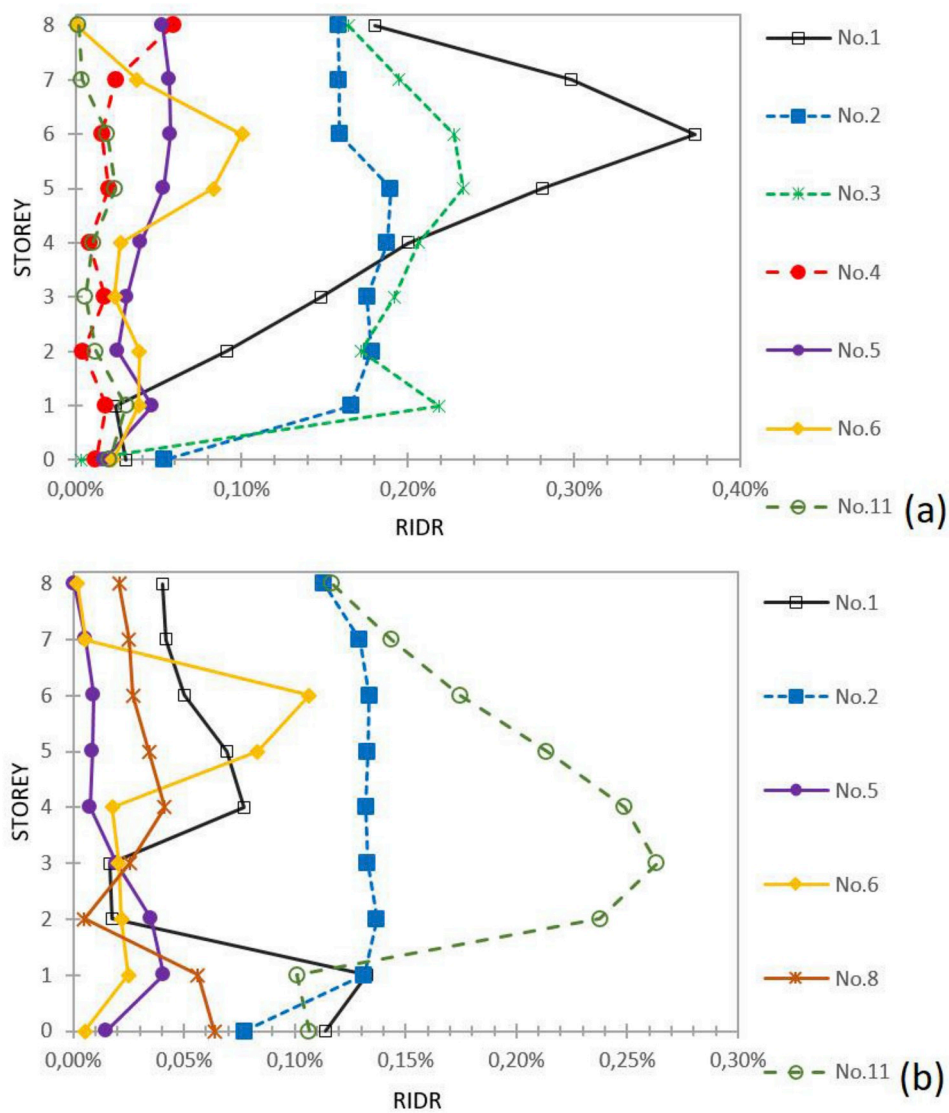

Fig. 22. RIDR responses of the 8-storey seesaw-braced (a) and buckling-restrained braced (b) steel structures (soil type D).

All authors certify that have seen and approved the manuscript being submitted. We warrant that the article is the Authors' original work. We warrant that the article has not received prior publication and is not under consideration for publication elsewhere. On behalf of all Co-Authors, the corresponding Author shall bear full responsibility for the submission.

Acknowledgement

This research project has been co-financed by the Operational Program 'Human Resources Development, Education and Lifelong Learning' and is co-financed by the European Union (European Social Fund) and Greek National funds.

Appendix A. Supplementary data

Supplementary data to this article can be found online at https://doi.org/10.1016/j.soildyn.2019.105925.

References

[1] Christidis AA, Dimitroudi EG, Hatzigeorgiou GD, Beskos DE. Maximum seismic displacements evaluation of steel frames from their post-earthquake residual deformation. Bull Earthq Eng 2013;11:2233–48.
[2] Loulelis D, Hatzigeorgiou GD, Beskos DE. Moment resisting frames under repeated earthquakes. Earthquakes Struct. 2012;3:231–48.
[3] Baiguera M, Vasdravellis G, Karavasilis TL. Dual seismic-resistant steel frame with high post-yield stiffness energy-dissipative braces for residual drift reduction. J Constr Steel Res 2016;122:198–212.
[4] Tzimas AS, Kamaris GS, Karavasilis TL, Galasso C. Collapse risk and residual drift performance of steel buildings using post-tensioned MRFs and viscous dampers in near-fault regions. Bull Earthq Eng 2016;14:1643–62.
[5] McCormick J, Aburano H, Ikenaga M, Nakashima M. Permissible residual deformation levels for building structures considering both safety and human elements. In: Proceedings of the 14th world conference on earthquake engineering; 2008. Paper ID 05-06-0071, Beijing, China.
[6] https://corebrace.com/.
[7] Qu Z, Kishiki S, Maida Y, Sakata H, Wada A. Seismic responses of reinforced concrete frames with buckling restrained braces in zigzag configuration. Eng Struct 2015;105:12–21.
[8] Erochko J, Christopoulos C, Tremblay R, Choi H. Residual drift response of SMRFs and BRB frames in steel buildings designed according to ASCE 7-05. J Struct Eng 2011;137:589–99.
[9] Ariyaratana CA, Fahnestock LA. Evaluation of buckling-restrained braced frame seismic performance considering reserve strength. Eng Struct 2011;33:77–89.
[10] Ghowsi AF, Sahoo DR. Seismic performance of bucking-restrained braced frames with varying beam-to-column connections. Int. J. Steel Struct. 2013;13:607–21.
[11] Flogeras AK, Papagiannopoulos GA. On the seismic response of steel buckling-restrained braced structures including soil-structure interaction. Earthquakes Struct. 2017;12:469–78.
[12] FEMA 695. Quantification of building seismic performance factors. Washington D. C: Federal Emergency Management Agency; 2009.
[13] Zaruma S, Fahnestock LA. Assessment of design parameters influencing seismic collapse performance of buckling-restrained braced frames. Soil Dyn Earthq Eng 2018;113:35–46.
[14] Özkiliç YO, Bozkurt MB, Topkaya C. Evaluation of seismic response factors for BRBFs using FEMA P695 methodology. J Constr Steel Res 2018;151:41–57.
[15] SEAOC. Seismic design recommendations. Sacramento, California: Structural Engineers Association of California; 2009.
[16] Kersting RA, Fahnestock LA, López WA. Seismic design of steel buckling restrained braced frames: a guide for practicing engineers. NIST GCR 15-917-34. Gaithersburg, MD: National Institute of Standards and Technology; 2015.
[17] AISC. Seismic provisions for structural steel buildings. Chicago, Illinois: American Institute of Steel Construction; 2016.
[18] EC 8. Eurocode 8 - design of structures for earthquake resistance, Part 1-1: general rules, seismic actions and rules for buildings. Brussels: European Committee for Standardization (CEN); 2009.
[19] Bosco M, Marino EM, Rossi PP. Design of steel frames equipped with BRBs in the framework of Eurocode 8. J Constr Steel Res 2015;113:43–57.
[20] Qiu CX, Zhu S. Performance-based seismic design of self-centering steel frames with SMA-based braces. Eng Struct 2017;130:67–82.
[21] Zahrai SM, Mousavi SA, Saatcioglu M. Analytical study on seismic behavior of proposed hybrid tension-only braced frames. Struct Des Tall Special Build 2017. https://doi.org/10.1002/tal.1310.
[22] Qiu C, Zhang Y, Li H, Qu B, Hou H, Tian L. Seismic performance of concentrically braced frames with non-buckling braces: a comparative study. Eng Struct 2018; 154:93–102.
[23] Papagiannopoulos GA. On the seismic behavior of tension-only concentrically braces steel structures. Soil Dyn Earthq Eng 2018;115:27–35.
[24] Chi P, Guo T, Peng Y, Cao D, Dong J. Development of a self-centering tension-only brace for seismic protection of frame structures. Steel Compos Struct 2018;26: 573–82.
[25] Kang JD, Tagawa H. Seismic performance of steel structures with seesaw energy dissipation systems using fluid viscoelastic dampers. Earthq Eng Struct Dyn 2013; 42:779–94.
[26] Kang JD, Tagawa H. Seismic performance of steel structures with seesaw energy dissipation systems using fluid viscous dampers. Eng Struct 2013;56:431–42.
[27] Kang JD, Tagawa H. Experimental evaluation of dynamic characteristics of seesaw energy dissipation system for vibration control of structures. Earthq Eng Struct Dyn 2014;43:1889–995.
[28] Katsimpini PS, Papagiannopoulos GA, Sfakianakis MG. On the seismic response and damping capacity of low-rise plane steel frames with seesaw system. Soil Dyn Earthq Eng 2018;107:407–16.
[29] Katsimpini PS, Papagiannopoulos GA, Askouni PK, Karabalis DL. Seismic response of low-rise 3-D steel structures equipped with the seesaw system. Soil Dyn Earthq Eng 2020;128:105877.
[30] EC 3. Eurocode 3 - design of steel structures, Part 1-1: general rules and rules for buildings. Brussels: European Committee for Standardization (CEN); 2009.
[31] EC 3. Eurocode 3 - design of structures with tension components, Part 1-11: general rules, seismic actions and rules for buildings. Brussels: European Committee for Standardization (CEN); 2009.
[32] SAP 2000. Static and dynamic finite element analysis of structures: version 19.0, Computers and Structures. 2016 [Berkeley, California].
[33] Bosco M, Marino EM. Design method and behavior factor for steel frames with buckling restrained braces. Earthq Eng Struct Dyn 2013;42:1243–63.
[34] ETABS. Integrated analysis and design of building systems: version 16.2.1, Computers and Structures. 2016 [Berkeley, California].
[35] Mulliken JS, Karabalis DL. Discrete model for dynamic through-the-soil coupling of 3-d foundations and structures. Earthq Eng Struct Dyn 1998;27:687–710.
[36] EC 8. Eurocode 8 - design of structures for earthquake resistance, Part 5: foundations, retaining structures and geotechnical aspects. Brussels: European Committee for Standardization (CEN); 2004.
[37] AISC. Seismic provisions for structural steel buildings. Chicago, Illinois: American Institute of Steel Construction; 2016.
[38] ASCE 41-17. Seismic evaluation and retrofit of existing buildings. Virginia, U.S.A: American Society of Civil Engineers; 2017.
[39] Kalkan E, Kwong NS. Pros and cons of rotating ground motion records to fault-normal/parallel directions for response history analysis of buildings. J Struct Eng 2014;140:04013062.
[40] Fontara I-KM, Kostinakis KG, Manoukas GE, Athanatopoulou AM. Parameters affecting the seismic response of buildings under bi-directional excitation. Struct Eng Mech 2015;53:957–79.
[41] Giannopoulos D, Vamvatsikos D. Ground motion records for seismic performance assessment: To rotate or not to rotate? Earthq Eng Struct Dyn 2018;47:2410–25.
[42] Karavasilis TL, Kerawala S, Hale E. Hysteretic model for steel energy dissipation devices and evaluation of a minimal-damage seismic design approach for steel buildings. J Constr Steel Res 2012;70. pp. 358–357.
[43] Zona A, Dall' Asta A. Elastoplastic model for steel buckling-restrained braces. J Constr Steel Res 2012;68:118–25.
[44] Speicher MS, Harris III JL. Collapse prevention seismic performance assessment of new buckling-restrained braced frames using ASCE 41. Eng Struct 2018;164: 274–89.